

# QCD parameters and SM-high precisions from $e^+e^- \rightarrow \text{Hadrons}$

Stephan Narison

*Laboratoire Univers et Particules de Montpellier (LUPM), CNRS-IN2P3,  
Case 070, Place Eugène Bataillon, 34095 - Montpellier, France*

*and  
Institute of High-Energy Physics of Madagascar (iHEPMAD)  
University of Ankatso, Antananarivo 101, Madagascar*

---

## Abstract

Using the PDG 22 compilation of the  $e^+e^- \rightarrow \text{Hadrons} \oplus$  the recent CMD3 data for the pion form factor and the value of gluon condensate  $\langle\alpha_s G^2\rangle$  from heavy quarkonia, we extract the value of the four-quark condensate:  $\rho\alpha_s\langle\bar{\psi}\psi\rangle^2 = (5.98 \pm 0.64) \times 10^{-4} \text{ GeV}^6$  and the dimension eight condensate:  $d_8 = (4.3 \pm 3.0) \times 10^{-2} \text{ GeV}^8$  from the ratio  $\mathcal{R}_{10}$  of Laplace sum rules to order  $\alpha_s^4$ . We show the inconsistency in using at the same time the standard SVZ value of the gluon and the vacuum saturation of the four-quark condensates. Using the previous values of the four-quark and  $d_8$  condensates, we re-extract  $\langle\alpha_s G^2\rangle$  from  $\mathcal{R}_{10}$  to be:  $(6.12 \pm 0.61) \times 10^{-2} \text{ GeV}^4$  in perfect agreement with the one from heavy quarkonia. We also use the lowest  $\tau$ -like decay moment  $\mathcal{R}_\tau^{ee}$  to extract the value of the QCD coupling. We obtain to  $\mathcal{O}(\alpha_s^4)$  the mean of FO (fixed order) and CI (contour improved) PT series within the standard OPE:  $\alpha_s(M_\tau) = 0.3385(50)(136)_{\text{sys}}$  where the last error is an added conservative systematic from the distance of the mean to the FO and CI central values. Assuming that the  $\alpha_s$ -coefficients of the PT series grow geometrically as observed in the calculated case, we obtain to  $\mathcal{O}(\alpha_s^5)$ :  $\alpha_s(M_\tau) = 0.3262(37)(78)_{\text{sys}}$ . These results lead to:  $\alpha_s(M_Z) = 0.1207(17)(3)$  [resp.  $0.1193(11)(3)$ ] to order  $\alpha_s^4$  [resp.  $\alpha_s^5$ ]. The corresponding value of the sum of the non-perturbative contribution at  $M_\tau$  is:  $\delta_{NP}^V(M_\tau) = (2.3 \pm 0.2) \times 10^{-2}$ . Reciprocally, using  $\alpha_s(M_\tau)$ ,  $\langle\alpha_s G^2\rangle$  and  $d_8$  as inputs, we test the stability of the value of the four-quark condensate obtained from the lowest  $\tau$ -like moment. We complete our analysis by updating our previous determinations of the lowest order hadronic vacuum polarization contributions to the lepton anomalies and to  $\alpha(M_Z^2)$ . We obtain in Table 3:  $a_\mu|_{l.o}^{hvp} = (7036.5 \pm 38.9) \times 10^{-11}$ ,  $a_\tau|_{l.o}^{hvp} = (3494.8 \pm 24.7) \times 10^{-9}$  and  $\alpha^{(5)}(M_Z)|_{had} = (2766.3 \pm 4.5) \times 10^{-5}$ . This new value of  $a_\mu$  leads to:  $\Delta a_\mu \equiv a_\mu^{exp} - a_\mu^{th} = (142 \pm 42_{th} \pm 41_{exp}) \times 10^{-11}$  which reduces the tension between the SM prediction and experiment.

**Keywords:** QCD spectral sum rules, QCD parameters, Hadron masses and couplings,  $\tau$ -decay, g-2.

---



---

*Email address:* snarison@yahoo.fr (Stephan Narison)

## 1. Introduction

Precise determinations of the QCD parameters are important inputs for testing the Standard Model (SM). Moreover, the study of hadronic properties necessitates a control of the non-perturbative effects where the exact solution is analytically lacking due to our poor knowledge of confinement. Some alternative approaches have been proposed such the numerical lattice simulations. Another approximate approach proposed by Shifman-Vainshtein and Zakharov (SVZ) [1]<sup>1,2</sup> is to parametrize the non-perturbative effects by a sum of vacuum condensates with increasing dimensions within the Operator Product Expansion (OPE).

In this paper, we shall extract some of these non-perturbative condensates and the QCD coupling from the  $e^+e^- \rightarrow \text{hadrons}$  data using the SVZ Laplace transform and the lowest  $\tau$ -decay moment sum rules. We complete the analysis for updating our previous determinations [17–21] of the lowest order hadronic vacuum polarization contributions to the lepton anomaly  $a_{\mu,\tau}$  and to the QED coupling  $\alpha(M_Z^2)$ .

## 2. The SVZ - anatomy of the two-point vector correlator

In this paper, we take the example of the hadronic two-point correlator built from the  $I = 1$  vector current :

$$J_H^\mu(x) = \frac{1}{2} [ : \bar{\psi}_u \gamma^\mu \psi_u - \bar{\psi}_d \gamma^\mu \psi_d : ]. \quad (1)$$

The two-point function reads:

$$\Pi_H^{\mu\nu}(q^2 \equiv -Q^2) = i \int d^4x e^{-iqx} \langle 0 | \mathcal{T} J_H^\mu(x) (J_H^\nu(0))^\dagger | 0 \rangle = -(g^{\mu\nu} q^2 - q^\mu q^\nu) \Pi_H(Q^2) \quad (2)$$

The corresponding SVZ-expansion reads:

$$8\pi^2 \Pi_H(-Q^2, m_q^2, \mu) = \sum_{D=0,2,4,\dots} \frac{C_D(Q^2, m_q^2, \mu) \langle O_D(\mu) \rangle}{(Q^2)^{D/2}}, \quad (3)$$

where  $\mu$  is the subtraction scale which separates the long and short distance dynamics and  $m_q$  is the quark mass. In addition to the usual perturbative contribution, there are QCD vacuum condensates  $\langle O_D(\mu) \rangle$  effects which are assumed by SVZ to approximate the not yet under good control QCD confinement.  $C_D(\mu)$  are separated calculable Wilson coefficients in perturbative theory (PT). The renormalization of the  $D = 4$  condensates has been studied in [22, 23], of  $D = 6$  in [24] and of  $D = 8$  in [25]. In this paper we assume that the observables which we shall look for are described with a good approximation by the condensates up to dimension  $D = 8$  and neglect the contribution of higher dimensions one. In this way, the  $D = 8$  condensates which we shall retain is an effective condensate which we expect to absorb into it the sum of the contributions of all higher dimension ones. Then, we shall be concerned with the following quantities:

---

<sup>1</sup>For reviews, see e.g. [4–16].

<sup>2</sup>The Laplace transform property of the SVZ Borel sum rule has been noticed by [2] while its non-relativistic form has been studied in [3].

- *D=0 perturbation theory*

The expression of the two-point function is known to order  $\alpha_s^3$  [26] and to order  $\alpha_s^4$  [27]. It reads for 3 flavours:

$$8\pi \text{Im}\Pi_H(t) = 1 + a_s + 1.6398a_s^2 - 10.2839a_s^3 - 106.8798a_s^4 + \mathcal{O}(a_s^5), \quad (4)$$

where :

$$a_s \equiv \frac{\alpha_s}{\pi} = \frac{2}{-\beta_1 \text{Log}(t/\Lambda^2)} + \dots, \quad (5)$$

where  $-\beta_1 = (1/2)(11 - 2n_f/3)$  is the first coefficient of the  $\beta$ -function and  $n_f$  is the number of quark flavours;  $\dots$  stands for higher order terms which can e.g. be found in [6]. We shall use the expression of  $\alpha_s$  up to order  $\alpha_s^3$  and the value  $\Lambda = (342 \pm 8)$  MeV for  $n_f = 3$  from the PDG average [43].

- *D=2 operators*

Within the standard OPE, the  $D = 2$  operators concern the quark mass squared which reads:

$$d_2|m_q \equiv C_2\langle O_2\rangle|_{m_q} = -3(\bar{m}_u^2 + \bar{m}_d^2) \left(1 + \frac{2}{3}a_s\right). \quad (6)$$

However, it was emphasized in Res. [28–31] that some unusual term due to tachyonic gluon mass related to the linear term of the QCD potential may appear in the OPE as a phenomenological parametrization of the non-calculated higher order PT terms and can be an alternative to the large  $\beta$ -UV renormalon approach. Its also appears in some ADS-QCD models [32, 33]. It reads [28]:

$$d_2|_{tach} \equiv C_2\langle O_2\rangle|_{tach} = \left(\frac{32}{2} - 8\zeta_3\right) \alpha_s \lambda^2 \log \frac{Q^2}{\mu^2}. \quad (7)$$

The value of the tachyonic mass extracted from the  $e^+e^- \rightarrow I=1$  hadrons data and  $\pi$  sum rules is [34–37]:

$$\alpha_s \lambda^2 \simeq -(7 \pm 3) \times 10^{-2} \text{ GeV}^2. \quad (8)$$

However, to avoid some misinterpretation of the result obtained in this paper, we shall not consider this term in our analysis but only show its effect in the sum rule.

- *D=4 light quark condensate*

Its value comes from the well-known Gell-Mann-Oakes Renner pion PCAC relation:

$$(m_u + m_d)\langle \bar{\psi}_u \psi_u + \bar{\psi}_d \psi_d \rangle = -m_\pi^2 f_\pi^2 : \quad f_\pi = 92.2 \text{ MeV}. \quad (9)$$

Its contribution to the two-point function reads:

$$d_4|_{\langle \bar{\psi}\psi \rangle} \equiv C_4\langle O_4\rangle|_{\langle \bar{\psi}\psi \rangle} = 4\pi^2 \left(1 + \frac{a_s}{3}\right) \langle m_u \bar{\psi}_u \psi_u + m_d \bar{\psi}_d \psi_d \rangle \quad (10)$$

- *D=4 gluon condensate*

It plays an important role in the heavy quark sector as the heavy quark vacuum condensate  $\langle \bar{Q}Q \rangle$  vanishes as the inverse of its mass  $1/M_Q$ . Its recent value from heavy quarkonia is [38]<sup>3</sup>:

$$\langle \alpha_s G^2 \rangle = (6.49 \pm 0.35) \times 10^{-2} \text{ GeV}^4, \quad (11)$$

which is 1.7 times the original SVZ estimate. This result consolidates the previous claims that its size has been underestimated [3, 12, 41, 42]. Its contribution is:

$$d_4|_{\langle G^2 \rangle} \equiv C_4 \langle O_4 \rangle |_{\langle G^2 \rangle} = \frac{\pi}{3} \langle \alpha_s G^2 \rangle \left( 1 + \frac{7}{6} a_s \right) \quad (12)$$

- *D=5 mixed quark-gluon condensate and D = 6 three-gluon condensate*

Notice that the  $D = 5$  mixed quark-gluon:  $\langle \bar{\psi} \sigma^{\mu\nu} \frac{\lambda_a}{2} G_{\mu\nu}^a \psi \rangle$  does not contribute in the chiral limit  $m_q = 0$  while the  $D = 6$  three-gluon:  $\langle g^3 f_{abc} G_{\mu\rho}^a G_{\nu}^{b,\rho} G_{\rho}^{c,\nu} \rangle$  do not contribute to leading order in  $\alpha_s$  [39] such that we shall neglect them.

- *D=6 four-quark condensate*

It has the generic form  $\langle \bar{\psi}_i \Gamma_1 \psi_j \bar{\psi}_k \Gamma_1 \psi_l \rangle$  where using a vacuum saturation assumption can be written in a simple way as  $\rho \langle \bar{\psi} \psi \rangle^2$  where  $\rho$  indicates the deviation from the vacuum saturation assumption. Present analysis indicates that

$$\rho \alpha_s \langle \bar{\psi} \psi \rangle^2 = 5.8(9) \times 10^{-4} \text{ GeV}^4, \quad (13)$$

indicating a huge violation of the vacuum saturation or factorization:

$$\alpha_s \langle \bar{\psi} \psi \rangle^2 |_{fac} = 1.0(9) \times 10^{-4} \text{ GeV}^4, \quad (14)$$

by a factor about 5.8. Notice that the four-quark condensate has a mild dependence of  $Q^2$  due to the almost cancellation of the  $\log(Q^2/\Lambda^2)$  of the running quark condensate and of the one of  $\alpha_s$ . Its contribution is:

$$d_6 \equiv C_6 \langle O_6 \rangle |_{\langle \bar{\psi} \psi \rangle^2} = -\frac{896}{81} \pi^3 \rho \alpha_s \langle \bar{\psi} \psi \rangle^2. \quad (15)$$

- *D=8 condensates*

We define for convenience:

$$d_8 \equiv C_8 \langle O_8 \rangle. \quad (16)$$

The contribution of the  $D = 8$  condensates has been computed in the chiral limit [40]. Higher dimensions operators ( $D \geq 10$ ) will be omitted as well as contributions due to the estimate of large order uncalculated terms.

---

<sup>3</sup>Different determinations from light and heavy quark channels are reviewed in this paper.

### 3. QCD parameters from $e^+e^- \rightarrow \text{I}=1$ hadrons data

We shall determine the QCD parameters from  $e^+e^- \rightarrow \text{I}=1$  hadrons data. In so doing, we extract the  $e^+e^- \rightarrow \text{I}=1$  hadrons data component from the compilation of the sum of the exclusive decays given by PDG [43] for the ratio :

$$R_{ee} = \frac{\sigma(e^+e^- \rightarrow \text{Hadrons})}{\sigma(e^+e^- \rightarrow \mu^+\mu^-)}. \quad (17)$$

For  $e^+e^- \rightarrow \pi\pi$ , we shall compare the PDG compiled data with the new CMD3 measurement of the pion form factor [44]. We take the data below  $E_{cm}=1.875$  GeV where they remain quite precise. Then we subdivide the data into three regions. More subdivisions will be done for extracting with a better accuracy the SM-high precision parameters.

- *Warnings*

- ◊ We assume that some issues related to the correlations of data and some other experimental technical subtleties have been considered in the PDG compilation.

- ◊ Along this paper, we shall use the Mathematica program FindFit with optimized  $\chi^2$  and the program NSolve for our numerical analysis.

- ◊ To be conservative, we shall fit separately the ensemble of high data points and low data points. Our final result will be the mean of these two extremal values.

- *Region from  $2m_\pi$  to  $0.993$  GeV*

We isolate the  $I = 1$  part by subtracting the  $\omega$  meson contribution and the shoulder around the peak due to the  $\omega - \rho$  mixing. Then, we fit the data using the optimized  $\chi^2$  Mathematica program *Findfit*. In so doing we fit separately the maximum and minimum values of each data points. To minimize the number of the free parameters, we use as input the value  $\Gamma(\rho \rightarrow e^+e^-)$  from PDG [43]. Then, we obtain the parameters:

$$\begin{aligned} \text{Set 1 : } \quad & \Gamma(\rho \rightarrow e^+e^-) = (7.03 + 0.04) \text{ keV} \implies M_\rho = 755.56 \text{ MeV}, \quad \Gamma_\rho^{\text{tot}} = 132.04 \text{ MeV}, \\ \text{Set 2 : } \quad & \Gamma(\rho \rightarrow e^+e^-) = (7.03 - 0.04) \text{ keV} \implies M_\rho = 755.65 \text{ MeV}, \quad \Gamma_\rho^{\text{tot}} = 131.92 \text{ MeV}, \end{aligned} \quad (18)$$

where the mass slightly differs from  $M_\rho = 775.5$  MeV quoted by PDG [43] obtained using a more involved parametrization of the pion form factor and including  $\rho - \omega$  mixing. The result corresponds to the small dashed region shown in Fig.1 from our conservative fitting procedure. We have not tried to add more parameters on the pion form factor to improve the quality of the fit which is satisfactory for our purpose. In the section of lepton anomalies where more precise fits are required, we shall improve the fitting procedure by subdividing the regions. We show for a comparison the new data from CMD3 on the pion form factor [44]. The new data are 2-3 times more precise than the one compiled by PDG [43] but the central values are approximately similar except in the low energy region where the CMD3 [44] data are slightly higher.

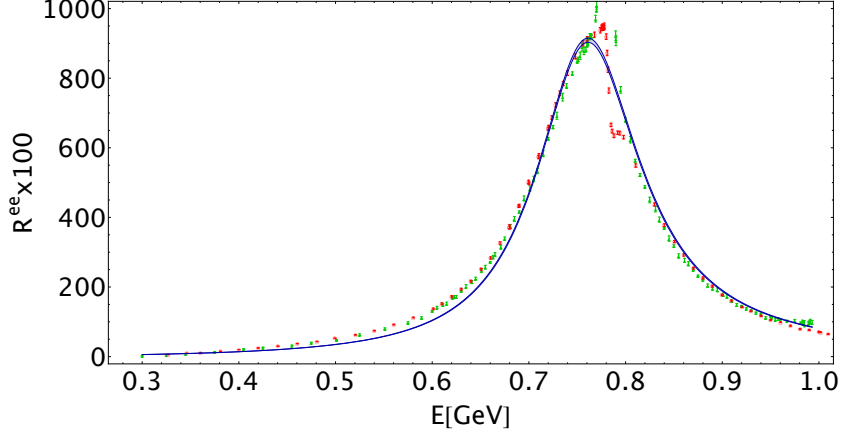


Figure 1: Fit of the data without  $\omega$  using a minimal Breit-Wigner parametrization of the PDG [43] compilation (green triangle) . A comparison with the new CMD3 [44] data is given (open red circle). .

- *Region from 0.993 to 1.5 GeV*

We fit the data using a simple interpolation program with polynomials. We subtract the  $3\pi$  backgrounds by using the  $SU(2)$  relation between the isoscalar and isovector states (a suppression 1/9 factor). We neglect the  $\bar{K}K$  contributions from isoscalar sources which, in addition to the  $SU(3)$  suppression factor is also suppressed by phase space. The fit is shown in Fig.2.

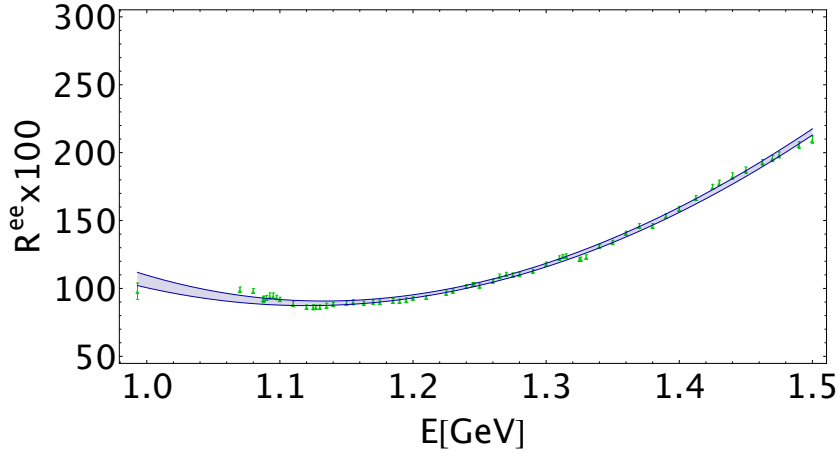


Figure 2: Fit of the data using a cubic polynomial interpolation formula.

- *Region from 1.5 to 1.875 GeV*

We use a Breit-Wigner fit for a  $\rho'$  meson. We obtain :

$$M_{\rho'} = 1.6 \text{ GeV} \text{ and } \Gamma(\rho' \rightarrow e^+e^-) = [10.5 \text{ (resp. 9.73)}] \text{ keV} \quad \Gamma_{\rho'}^{\text{tot}} = [720 \text{ (resp. 694)}] \text{ MeV}, \quad (19)$$

from the high (resp. low) data points. The fit is shown in Fig. 3.

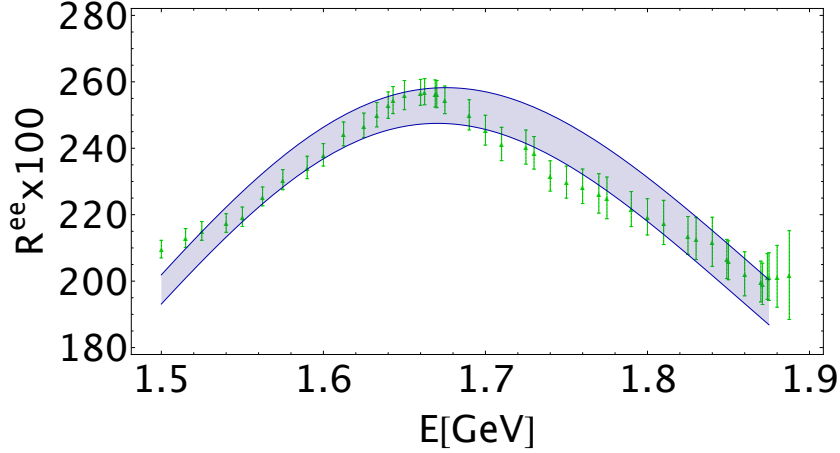


Figure 3: Fit of the data using a minimal Breit-Wigner parametrization.

#### 4. The (inverse) Laplace sum rules

The sum rule reads [1–3, 12]:

$$\begin{aligned}\mathcal{L}_0^c(\tau, \mu) &\equiv \lim_{\substack{Q^2, n \rightarrow \infty \\ n/Q^2 \equiv \tau}} \frac{(-Q^2)^n}{(n-1)!} \frac{\partial^n \Pi}{(\partial Q^2)^n} = \int_{t>}^{t_c} dt e^{-t\tau} R_{ee}^{I=1}(t, \mu) \\ \mathcal{R}_{10}^c(\tau) &\equiv \frac{\mathcal{L}_1^c}{\mathcal{L}_0^c} = \frac{\int_{t>}^{t_c} dt e^{-t\tau} t R_{ee}^{I=1}(t, \mu)}{\int_{t>}^{t_c} dt e^{-t\tau} R_{ee}^{I=1}(t, \mu)},\end{aligned}\quad (20)$$

where  $\tau$  is the LSR variable,  $t >$  is the hadronic threshold. Here  $t_c$  is the threshold of the “QCD continuum” which parametrizes, from the discontinuity of the Feynman diagrams, the spectral function  $\text{Im } \Pi_H(t, m_q^2, \mu^2)$ .  $m_q$  is the quark mass and  $\mu$  is an arbitrary subtraction point. The spectral function is related through the optical theorem to the isovector part of the ratio  $R_{ee}^{I=1}$  defined as in Eq. 17 as:

$$R_{ee}^{I=1} = \left(\frac{3}{2}\right) 8\pi \text{Im} \Pi_H(t). \quad (21)$$

Due to its superficial convergence, the Laplace sum rule obeys the homogeneous renormalization group equation (RGE) [2]

$$\left\{ -\tau \frac{\partial}{\partial \tau} + \beta(\alpha_s) \frac{\partial}{\partial \alpha_s} - \sum_i [1 + \gamma(\alpha_s) x_i] \frac{\partial}{\partial x_i} \right\} \mathcal{L}_n(\tau), \quad (22)$$

with  $x_i \equiv m_i(\mu)/\mu$  and  $\beta(\alpha_s), \gamma(\alpha_s)$  are the  $\beta$  function associated to the renormalization of  $\alpha_s$  and anomalous quark mass renormalization in the  $\overline{MS}$  scheme. The natural solution to this RGE is the choice  $\mu^2 = 1/\tau$ . The QCD expression of the first moment and the ratio of moments read:

$$\begin{aligned}\mathcal{L}_0^{qcd}(\tau) &= \tau^{-1} \frac{3}{2} \left[ 1 + a_s + a_s^2 (1.6398 - \frac{\beta_1}{2} \gamma_E) + \mathcal{O}(\alpha_s^3) + d_2 \tau + d_4 \tau^2 + \frac{d_6}{2} \tau^3 + \frac{d_8}{6} \tau^4 \right], \\ \mathcal{R}_{10}^{qcd}(\tau) &= \tau^{-1} \left[ 1 + \beta_1 a_s^2 + \mathcal{O}(\alpha_s^3) - d_2 \tau - 2d_4 \tau^2 - \frac{3}{2} d_6 \tau^3 - \left( \frac{2}{3} d_8 - d_4^2 \right) \tau^4 \right],\end{aligned}\quad (23)$$

where terms due to the Laplace operator in the PT corrections are explicitly shown. Thanks to the exponential weight, the previous sum rule improvements enhance the low energy contribution to the spectral integral which is accessible experimentally. The PT corrections to the ratio of moments  $\mathcal{R}_{10}$  start to order  $\alpha_s^2$  which renders it a good observable for extracting the non-perturbative condensates. Using the  $e^+e^- \rightarrow \text{Hadrons}$  data, Ref. [42] have used  $\mathcal{R}_{10}$  to extract the condensates and obtained (notice the different normalizations):

$$d_4 = (3.45 \pm 0.85) \times 10^{-2} \text{ GeV}^4, \quad d_6 = (0.12 \pm 0.04) \times 10^{-2} \text{ GeV}^6, \quad d_8 = (2.9 \pm 2.4) \text{ GeV}^8, \quad (24)$$

where the value of  $d_8$  is not conclusive while the one of  $d_4$  and  $d_6$  lead to the values:

$$\langle \alpha_s G^2 \rangle = (3.29 \pm 0.81) \times 10^{-2} \text{ GeV}^4 \quad \rho \langle \bar{\psi}\psi \rangle^2 = (3.5 \pm 1.16) \times 10^{-4} \text{ GeV}^6. \quad (25)$$

The value of  $\langle \alpha_s G^2 \rangle$  agrees with the original SVZ[1] value of  $3.8 \times 10^{-2} \text{ GeV}^4$  while the value of the four-quark condensate is larger by a factor 3 compared to the factorization estimate in Eq. 14. However, a more recent analysis using  $R_{10}$  and the  $\tau$ -like decay sum rules for the  $I = 1$  hadrons data lead to [35, 36]:

$$\langle \alpha_s G^2 \rangle = (7.1 \pm 0.7) \times 10^{-2} \text{ GeV}^4 \quad \rho \langle \bar{\psi}\psi \rangle^2 = (5.8 \pm 0.9) \times 10^{-4} \text{ GeV}^6, \quad d_8 = -(0.38 \pm 0.15) \text{ GeV}^8. \quad (26)$$

One should note from Eqs. 25 and 26 that there is a discrepancy by a factor of about 2 for the estimate of  $\langle \alpha_s G^2 \rangle$  and  $\rho \langle \bar{\psi}\psi \rangle^2$  but both results indicate a huge violation of the four-quark vacuum saturation.

In the following, our aim is to try to clarify the contradictory results from the SVZ-like sum rules and from  $\tau$ -decay moments using the example of vector current channel and the lowest moments and their ratio.

## 5. Fixing the value of the QCD continuum threshold $t_c$

First, we have to fix the value of the QCD continuum threshold  $t_c$  above which we shall parametrize the spectral function by its QCD expression given in Eq. 4.

### • $t_c$ from the moment $\mathcal{L}_0^{ee}$

We request that the data and the perturbative QCD expression of the moment  $\mathcal{L}_0^{ee}$  coincides for the sum rule variable  $\tau \leq 0.7 \text{ GeV}^{-2}$  where the non-perturbative effects to the QCD expression are expected to be negligible while the difference between the QCD contribution with the data one without a QCD continuum remains positive. Using the Mathematica optimized  $\chi^2$  fit program FindFit. We obtain to order  $\alpha_s^4$  accuracy :

$$t_c = (4.74 \sim 4.93) \text{ GeV}^2, \quad (27)$$

where  $t_c = 4.74$  (resp. 4.93)  $\text{GeV}^2$  corresponds to the fit of the low (resp. high) set of values of the data points. The result of the analysis is shown in Fig.4. We have improved the fit for the low data points by adjusting manually the value of  $t_c$ . Then, we arrive at the conservative range of values :

$$t_c = (4 \sim 5) \text{ GeV}^2, \quad (28)$$



which we shall use for the forthcoming analysis.

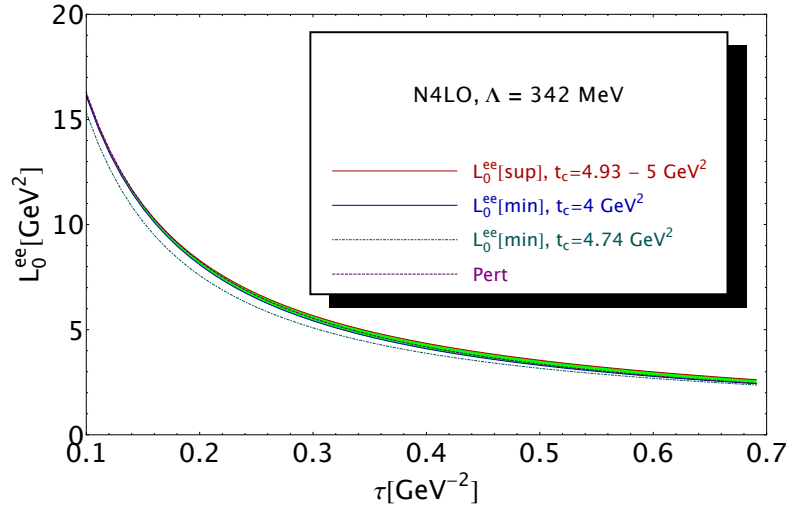


Figure 4: Comparison of the QCD expression of  $\mathcal{L}_0^{ee}$  with the data for the obtained value of  $t_c$  given in Eq. 28

- *Comments and comparison*

It is informative to compare this result with the one required by FESR for a duality between the experimental and QCD side of the sum rule [41]:

$$F_0(t_c) \equiv \int_0^{t_c} dt R_{ee}^{I=1}(t) = \frac{3}{2} t_c \left[ 1 + a_s(t_c) + a_s^2(t_c) \left( 1.6398 - \frac{\beta_1}{2} \right) + \dots \right] \quad (29)$$

where  $\dots$  comes from a numerical integration of the integral at order  $\alpha_s^3$ . The analysis for the ratio

$$R_0^{fesr} \equiv \frac{F_0^{data}}{F_0^{qcd}} \quad (30)$$

is shown in Fig. 5 from which one can deduce to order  $\alpha_s^3$  the duality region:

$$t_c^{fesr} = (5.1 \sim 5.6) \text{ GeV}^2, \quad (31)$$

The value in Eq. 31 is higher than the value around  $2.1 \text{ GeV}^2$  obtained in Ref. [41]. We interpret the origin of this discrepancy as due to the effect of the old data and of its parametrization in the  $\rho'$ -region. This value does not also justify the choice  $t_c = 1.55 \text{ GeV}^2$  used in Ref. [46] for the unpinched moment which is equivalent to the lowest degree of FESR used here.

## 6. QCD condensates from the ratio $\mathcal{R}_{10}$ of Laplace sum rules moments

We shall extract the condensates from the ratio of moments which has the advantage to be less sensitive to the PT  $\alpha_s$  corrections which tends to cancel out in the ratio.

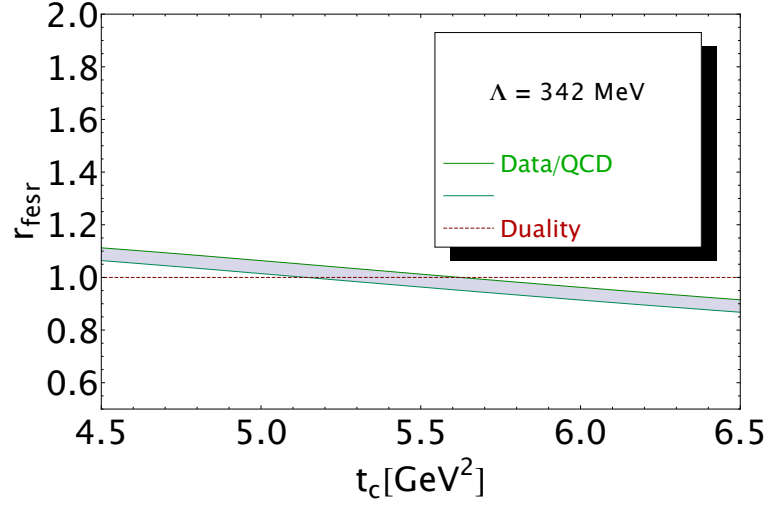


Figure 5: Variation of the ratio in Eq. 30 versus  $t_c$ .

- $\langle \alpha_s G^2 \rangle$  and  $d_6$  from the ratio of moments  $\mathcal{R}_{10}$  to order  $\alpha_s^2$

We attempt to extract the gluon condensate  $\langle \alpha_s G^2 \rangle$  and the  $D = 6$  four-quark condensate from the ratio of moments to order  $\alpha_s^2$  by neglecting the contributions of  $D \geq 8$  ones. The analysis is shown in Fig. 6 versus the sum rule variable  $\tau$ . The green curves delimit the value of  $\langle \alpha_s G^2 \rangle$  and the red ones the value of  $d_6$ . We notice that there is no stability in  $\tau$  such that the analysis is unconvulsive. The results obtained from a fit by LNT in Ref. [42] are shown by the full triangle ( $\langle \alpha_s G^2 \rangle$ ) and open circle ( $d_6$ ).

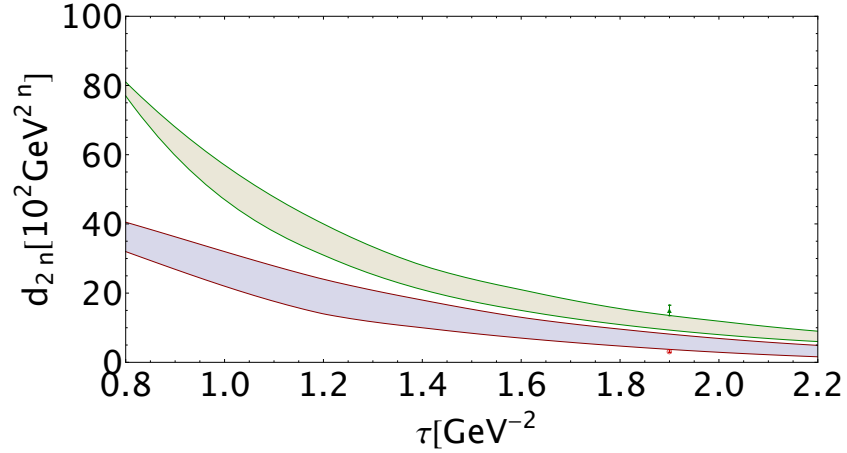


Figure 6: Two-parameter fit of  $\langle \alpha_s G^2 \rangle$  and  $-d_6$  from the ratio of moments  $\mathcal{R}_{10}$ .

- $d_6$  and  $d_8$  from the ratio of moments  $\mathcal{R}_{10}$  to order  $\alpha_s^2$

We impose more constraints on the parameters by using as input the value of the gluon condensate given in Eq. 11 from heavy quark sum rules<sup>4</sup>. As mentioned in the introduction, we shall truncate the OPE at  $D = 8$  and assume that the  $D = 8$  condensate is an effective condensate which absorbs into it all higher dimension ones. One also should note that looking for a combination of these high-dimension condensates to have a physical meaning is a difficult task as they mix under renormalization [24].

Given the previous value of  $t_c$  in Eq. 28, we study the effect of the Laplace sum rule variable  $\tau$  on the result. This is shown in Fig. 7. One can observe a  $\tau$ -stability at  $\tau \simeq 2.6$  to  $3.4 \text{ GeV}^{-2}$  which

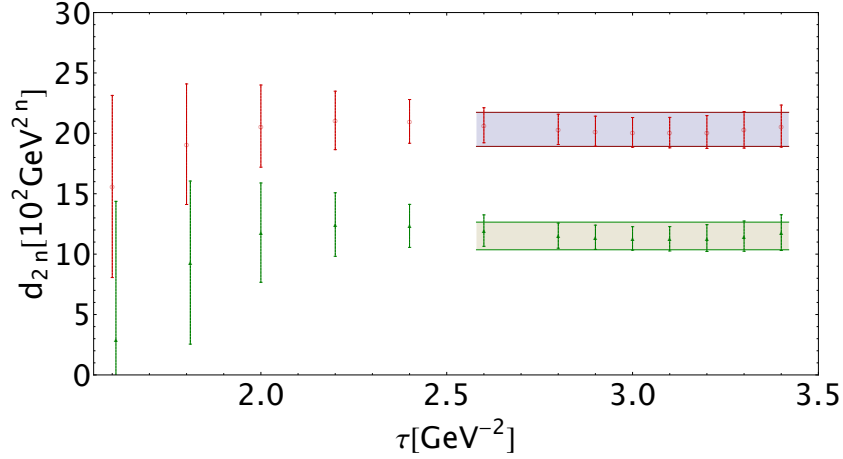


Figure 7: Two-parameter fit of  $-d_6$  and  $+d_8$  to order  $\alpha_s^2$  for a given value of  $\langle \alpha_s G^2 \rangle$  from Eq. 11.

corresponds to the values:

$$d_6 = -(20.1 \pm 1.3) \times 10^{-2} \text{ GeV}^6, \quad d_8 = (11.3 \pm 1.1) \times 10^{-2} \text{ GeV}^8 \quad (32)$$

at order  $\alpha_s^2$ . As a final value, we consider the average of different results obtained in the region  $\tau \simeq 2.6$  to  $3.4 \text{ GeV}^{-2}$  around this minimum. We deduce (shaded region):

$$d_6 = -(20.3 \pm 1.4) \times 10^{-2} \text{ GeV}^6, \quad d_8 = (11.5 \pm 1.2) \times 10^{-2} \text{ GeV}^8. \quad (33)$$

- *QCD PT corrections to order  $\alpha_s^4$*

One can include higher order terms by using the expression of  $\mathcal{L}_0$  to order  $\alpha_s^4$  [45] :

$$\mathcal{L}_0^{PT}(\tau) = \tau^{-1} \left[ 1 + a_s + 2.93856 a_s^2 + 6.2985 a_s^3 + 22.2233 a_s^4 \right], \quad (34)$$

and taking its derivative in  $\tau$  to get  $\mathcal{L}_1(\tau)$  and then their ratio  $\mathcal{R}_{10}(\tau)$ . We use the expression of  $\alpha_s$  to order  $\alpha_s^3$  given e.g. in Eq. 11.66 of [5]:

$$a_s(\tau) = a_s^{(0)} \left\{ 1 - a_s^{(0)} \frac{\beta_2}{\beta_1} l_\tau + \left( a_s^{(0)} \right)^2 \left[ \log^2(l_\tau) - \left( \frac{\beta_2}{\beta_1} \right)^2 \log(l_\tau) - \left( \frac{\beta_2}{\beta_1} \right)^2 + \frac{\beta_3}{\beta_1} \right] + \mathcal{O}(a_s^3) \right\}, \quad (35)$$

<sup>4</sup>A 3-parameter fit does not lead to a conclusive result.

where :  $l_\tau \equiv -\log \tau \Lambda^2$ ,  $a_s^{(0)} \equiv 2/(\beta_1 l_\tau)$  and, for three flavours:

$$\beta_1 = -9/2, \quad \beta_2 = -8, \quad \beta_3 = -20.1198. \quad (36)$$

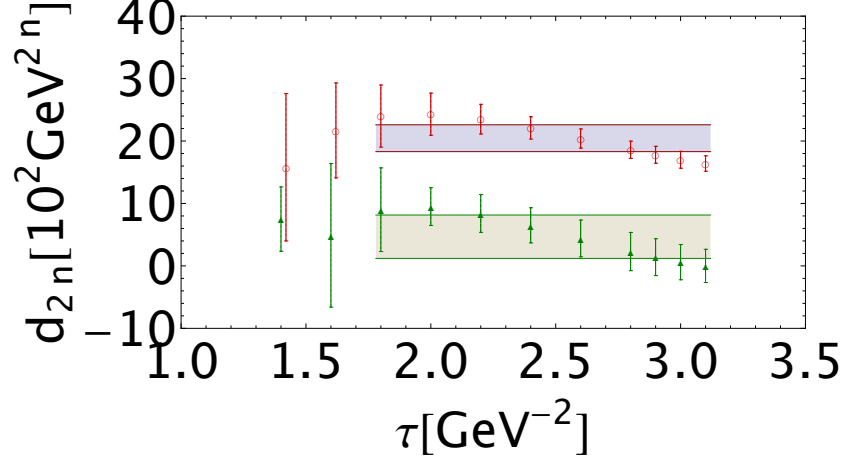


Figure 8: Two-parameter fit of  $-d_6$  and  $+d_8$  to order  $\alpha_s^4$  for a given value of  $\langle \alpha_s G^2 \rangle$  from Eq. 11.

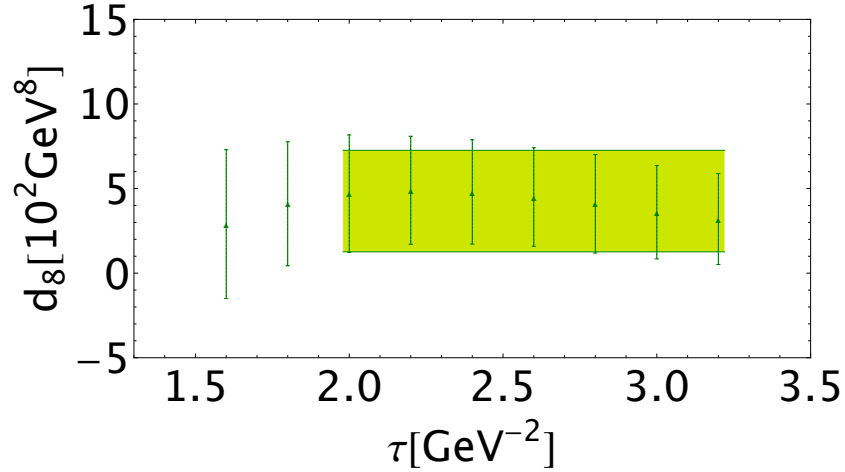


Figure 9: One-parameter fit of  $d_8$  to order  $\alpha_s^4$  for a given value of  $\langle \alpha_s G^2 \rangle$  from Eq. 11 and  $d_6$  from Eq. 37.

- *Extraction of  $d_6$  and  $d_8$  to order  $\alpha_s^4$*

We show in Fig. 8 the results from a two-parameter fit to order  $\alpha_s^4$ . By comparing Figs. 7 and 8, one can notice that the  $\alpha_s^4$ -term destabilizes the  $\tau$ -behaviour of  $d_6$  and  $d_8$ . A least square fit of the points between 1.8 and 3.2  $\text{GeV}^{-2}$  where the determinations are more precise gives:

$$d_6 = -(20.5 \pm 2.2) \times 10^{-2} \text{ GeV}^6, \quad d_8 = (4.7 \pm 3.5) \times 10^{-2} \text{ GeV}^8. \quad (37)$$

The value of  $d_6$  remains unchanged from  $\alpha_s^2$  to  $\alpha_s^4$  which is not the case of  $d_8$  which has decreased by about a factor 2.5! Then, we try to improve the determination of  $d_8$  by using  $d_6$  as input in addition to the previous input parameters. The analysis shown in Fig.9 indicates a much better stability though we do not (unfortunately) gain much on the accuracy. We obtain:

$$d_8 = (4.3 \pm 3.0) \times 10^{-2} \text{ GeV}^8. \quad (38)$$

which we consider as a final result for  $d_8$ . However, this low value of  $d_8$  compared to the one obtained at order  $\alpha_s^2$  in Eq. 33 is a good news for QCD sum rules users. It (a posteriori) justifies the neglect of high-dimension condensates in the analysis which gives a good description of different hadron parameters when only the dimension  $D \leq 6$  condensates are retained in the OPE.

From the value of  $d_6$  in Eq. 37, one can deduce the value of the four-quark condensate determined at order  $\alpha_s^4$ :

$$\rho \langle \bar{\psi}\psi \rangle^2 = (5.98 \pm 0.64) \times 10^{-4} \text{ GeV}^6, \quad (39)$$

which (agreably) confirms the value in Eq. 13 from heavy quarkonia and the average of different determinations quoted in [38].

- *A second attempt to extract  $\langle \alpha_s G^2 \rangle$  to order  $\alpha_s^4$   
 $\diamond \langle \alpha_s G^2 \rangle$  and  $d_6$  from a two-parameter fit*

First, we repeat the analysis done previously and neglect the  $d = 8$  condensates. One can notice (see Fig. 10) that the presence of the  $\alpha_s^4$  term leads in this case to  $\tau$ -stability (minimum) at  $\tau \simeq 2.4 \text{ GeV}^{-2}$  from which we extract the optimal values:

$$\langle \alpha_s G^2 \rangle = (5.9 \pm 2.6) \times 10^{-2} \text{ GeV}^4, \quad d_6 = -(17.1 \pm 4.1) \times 10^{-2} \text{ GeV}^6, \quad (40)$$

where the main error is due to the data fitting procedure. These values agree with the determination of  $\langle \alpha_s G^2 \rangle$  from heavy quarkonia in Eq. 11 and with the one of  $d_6$  in Eq. 37 but inaccurate.

- $\diamond \langle \alpha_s G^2 \rangle$  from a one-parameter fit

To improve the determination of  $\langle \alpha_s G^2 \rangle$ , we use as input the value of  $d_6$  in Eq. 37 and include  $d_8$  from Eq. 38. The analysis is shown in Fig. reffig:d4. We deduce at the stability point  $\tau \simeq 1.5 \text{ GeV}^{-2}$ :

$$\langle \alpha_s G^2 \rangle = (6.12 \pm 0.61) \times 10^{-2} \text{ GeV}^4, \quad (41)$$

which improves the result in Eq. 40. Combining this value with the one from heavy quarkonia in Eq. 11, we deduce the average:

$$\langle \alpha_s G^2 \rangle = (6.40 \pm 0.30) \times 10^{-2} \text{ GeV}^4, \quad (42)$$

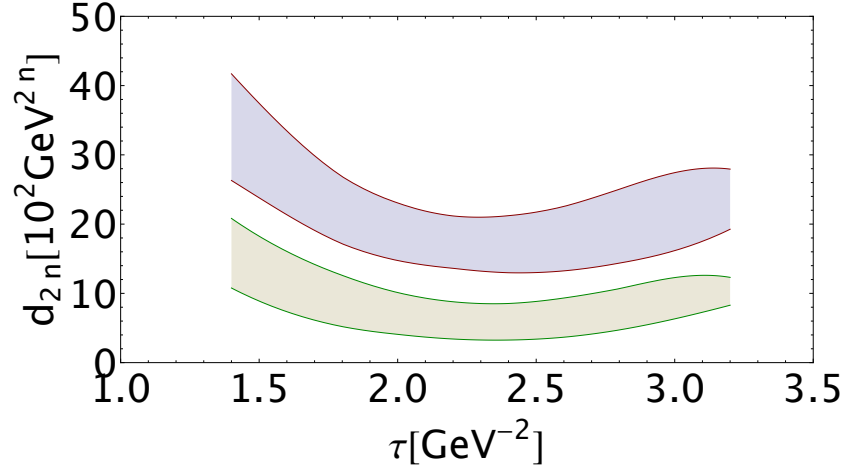


Figure 10: Two-parameter fit of  $\langle \alpha_s G^2 \rangle$  (lower curves) and  $d_6$  (upper curves) to order  $\alpha_s^4$ .

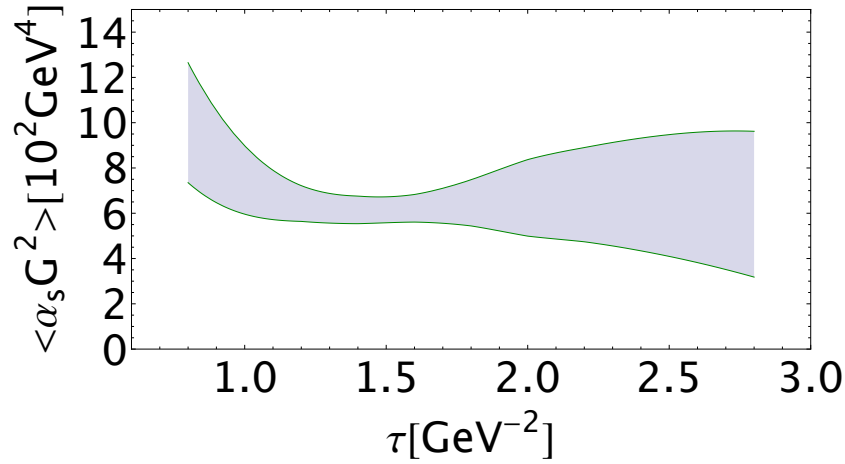


Figure 11: One-parameter fit of  $\langle \alpha_s G^2 \rangle$  to order  $\alpha_s^4$  using  $d_6$  in Eq. 37 and  $d_8$  from Eq. 16.

- *Comparison with LNT [42]*

We consider this result as an improvement of the one of LNT in Ref. [42] (notice a slightly different normalization):

$$d_6|_{lnt} = -(12.7 \pm 4.2) \times 10^{-2} \text{ GeV}^6, \quad d_8|_{lnt} = (27 \pm 24) \times 10^{-2} \text{ GeV}^8 \quad (43)$$

where the same ratio of moments has been used with a different strategy and data. The lower value of  $d_6$  is correlated to the low value of  $\langle \alpha_s G^2 \rangle$  obtained by LNT (see Fig.6).

- *Comparison with FESR [41]*

It is informative to compare this result with the one from FESR using  $e^+e^- \rightarrow \text{hadrons}$  data:

$$d_6 = \int_0^{t_c} dt t^2 R_{ee}^{I=1}(t) - \left(\frac{3}{2}\right) \frac{t_c^3}{3} \left[ 1 + a_s + a_s^2 \left( 1.6398 - \frac{\beta_1}{6} \right) + \dots \right], \quad (44)$$

which is interesting as it can disentangle the contributions of the condensates having a given dimension. One obtains [41]:

$$d_6|_{fesr} = -(0.33 - 0.55) \text{ GeV}^6, \quad (45)$$

where the order of magnitude and the sign agree with the previous estimate. However, we have attempted to rederive the FESR result and noticed that it is quite sensitive to the parametrization of the data at high-energy and to the corresponding value of  $t_c$  where  $d_6$  behaves as  $t_c^3$  in Eq. 31 such that our analysis has lead to an unconvulsive result. We should notice that the FESR needs a fine tuning for extracting the small  $d_6$  number from the difference of two big quantities. Similar comments apply for the extraction of the gluon condensate from the FESR:

$$d_4 = \left(\frac{3}{2}\right) \frac{t_c^2}{2} \left[ 1 + a_s + a_s^2 \left( 1.6398 - \frac{\beta_1}{4} \right) + \dots \right] - \int_0^{t_c} dt t R_{ee}^{I=1}(t) - . \quad (46)$$

It has been found that [41]:

$$\langle \alpha_s G^2 \rangle|_{fesr} \simeq (7 \sim 18) \times 10^{-2} \text{ GeV}^4. \quad (47)$$

Despite its inaccuracy, the range of value of the gluon condensate agrees with the one from different channels in Eq. 11 but disfavours the negative value from  $\tau$ -decay moments using CI [49, 50]. The inaccuracy of the FESR result also comes from the  $t_c^2$  dependence for its extraction.

- *Comparison with  $\tau$ -decay moments*

Different groups [46–51] have worked with a set of moments introduced in Ref. [52] and its variants which are a generalization of the original lowest  $\tau$ -decay rate moment used by BNP [53, 54]. Fitting three / four free parameters  $(\alpha_s, d_4, d_6, \dots)$ , the authors obtain results which vary in a large range. We compare our results with the ones from the vector component analysis.

- ◊ *Gluon condensate  $\langle \alpha_s G^2 \rangle$*

Its extraction is affected by the way of truncating the QCD series. Within the standard OPE, it can become negative for CI. Its values from different groups given in Table 1 vary in a large range which may indicate that  $\tau$ -decay like-moments are not a good tools for extracting  $\langle \alpha_s G^2 \rangle$ . We take the values from Table 1 of Ref. [49] which is consistent with the fact that we neglect the  $D \geq 10$  condensate contributions.

- ◊  *$d_6$  and  $d_8$  condensates*

Their determinations from  $\tau$ -like moments are compiled in Table 1. One can notice that, unlike the gluon condensate, they are less affected by the truncation of the PT series. Our values given in Eq. 37 are in the range of these values though the size of our  $d_8$  is about half.

$\langle\alpha_s G^2\rangle$	$-d_6$	$d_8$	PT series	Refs.
$0.67 \pm 0.89$	$15.2 \pm 2.2$	$22.3 \pm 2.5$	FO	ALEPH [47]
$5.34 \pm 3.64$	$14.2 \pm 3.5$	$21.3 \pm 2.5$	FO	OPAL [48]
$0.8^{+0.7}_{-1.4}$	$32^{+8}_{-5}$	$50^{+4}_{-7}$	FO	[49]
$0.31 \pm 2.45$	$13.5 \pm 1.8$	$20.0 \pm 1.6$	CI	OPAL [48]
$-1.57 \pm 0.94$	$14.7 \pm 1.1$	$20.4 \pm 1.3$	CI	ALEPH [50]
$-0.8^{+0.7}_{-0.7}$	$35 \pm 3$	$49^{+4}_{-5}$	CI	[49]

Table 1: Values of the QCD condensates of dimension  $D = 2n$  in units of  $10^{-2} \text{ GeV}^{2n}$  from  $\tau$ -like decays.

- *Correlated values of  $d_6$  and  $d_8$  versus  $\langle\alpha_s G^2\rangle$*

We show in Fig. 12 the behaviour of  $d_6$  and  $d_8$  versus  $\langle\alpha_s G^2\rangle$ . One can notice that:

◊ The value of the four-quark condensate estimated from factorization is inconsistent with the SVZ value of the gluon condensate.

◊ The ratio:

$$r_{46} \equiv \frac{\rho\langle\bar{\psi}\psi\rangle^2}{\langle\alpha_s G^2\rangle} \approx 0.9 \times 10^{-2} \text{ GeV}^2, \quad (48)$$

is almost constant. The value of  $r_{46}$  obtained here has also been obtained from different approaches [41, 42, 55–57] independently on the absolute size of the extracted condensates and on the kind of methods. However, we notice that the  $\tau$ -like moments values given in Table 1 do not fulfill such relations.

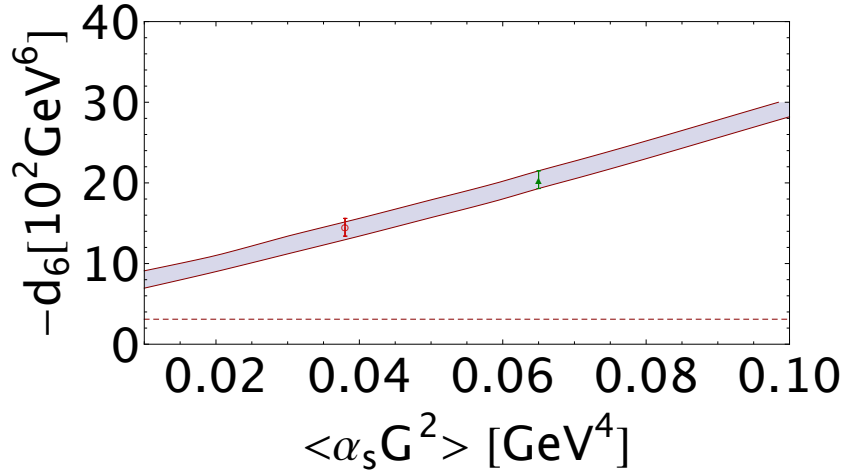


Figure 12: Correlated values of  $d_6$  and  $d_8$  versus  $\langle\alpha_s G^2\rangle$ . The dashed horizontal line is the value of  $d_6$  estimated from factorization of the four-quark condensate. The red (resp. olive) point corresponds to the value of  $\langle\alpha_s G^2\rangle$  given by SVZ and by Eq. 11.



## 7. Confronting theory and experiment for $\mathcal{R}_{10}^{ee}$ and $\mathcal{L}_0^{ee}$

Using as input the previous values of the condensates and the value of  $\alpha_s$  from PDG, we compare the QCD and experimental sides of  $\mathcal{R}_{10}$  and  $\mathcal{L}_0$  which we show in Figs. 13 and 14.

### • Ratio of moments $\mathcal{R}_{10}^{ee}$

We show the QCD predictions for different truncation of the OPE in Fig. 13. We observe that:

◊ For  $\tau \leq 1.5 \text{ GeV}^{-2}$ , the truncation of the OPE up to  $D = 6$  gives a good description of the data where we have a minimum. The presence of minimum or inflexion point is expected for an approximate QCD series as discussed in the example of an harmonic oscillator [3, 5, 6, 12]. The use of the standard SVZ value of the gluon condensate  $\oplus$  the value of the four-quark condensate estimated using the factorization assumption underestimates the data. However, the simultaneous use of the SVZ standard value  $\oplus$  the factorization (combination often used in the QCD sum rules literature) is inconsistent from the result of simultaneous two-parameter fit shown in the previous section and in Fig. 12.

◊ The inclusion of the  $D = 8$  condensate enlarges the region of agreement between the QCD prediction and the experiment until  $\tau = 2.5 \text{ GeV}^{-2}$  where the  $\rho$ -meson mass is reached and where, exceptionally, the PT series for the spectral function still make sense.

◊ We complete the analysis by adding the tachyonic gluon mass beyond the SVZ-expansion. We see that it tends to decrease the agreement with the data but the effect is (almost) negligible within our precision.

### • Lowest moment $\mathcal{L}_0^{ee}$

This moment has been used in Refs. [35, 58] to estimate  $\alpha_s$  and the QCD condensates.

◊ We have tried to extract these parameters using  $\mathcal{L}_0^{ee}$  but the results are unconvulsive. Contrary to the case of  $\mathcal{R}_{10}^{ee}$ , we notice an important sensitivity of the results on the truncation of the PT series. This problem can be evaded if one uses the  $\pi^2$  resummation of the higher order term where the PT series converges faster [59]. However, we also remark that the determination from the low and high sets of data vary in a large range leading to a very inaccurate result.

◊ Therefore, we just use the previous values of  $\alpha_s$  from the PDG average [43],  $\langle \alpha_s G^2 \rangle$  from Eq. 11 and  $d_4$  and  $d_6$  obtained in the previous section and compare the experimental and theoretical  $\tau$ -behaviour of the lowest moment  $\mathcal{L}_0^{ee}$  in Fig. 14.

◊ We observe that the effect of the:

- Tachyonic gluon mass, if any, is quite large for  $\tau \geq 0.6 \text{ GeV}^{-2}$ .
- $D = 8$  condensate is relatively small due to the  $(1/6)$  factor suppression induced by the exponential weight for the Laplace / Borel sum rule.

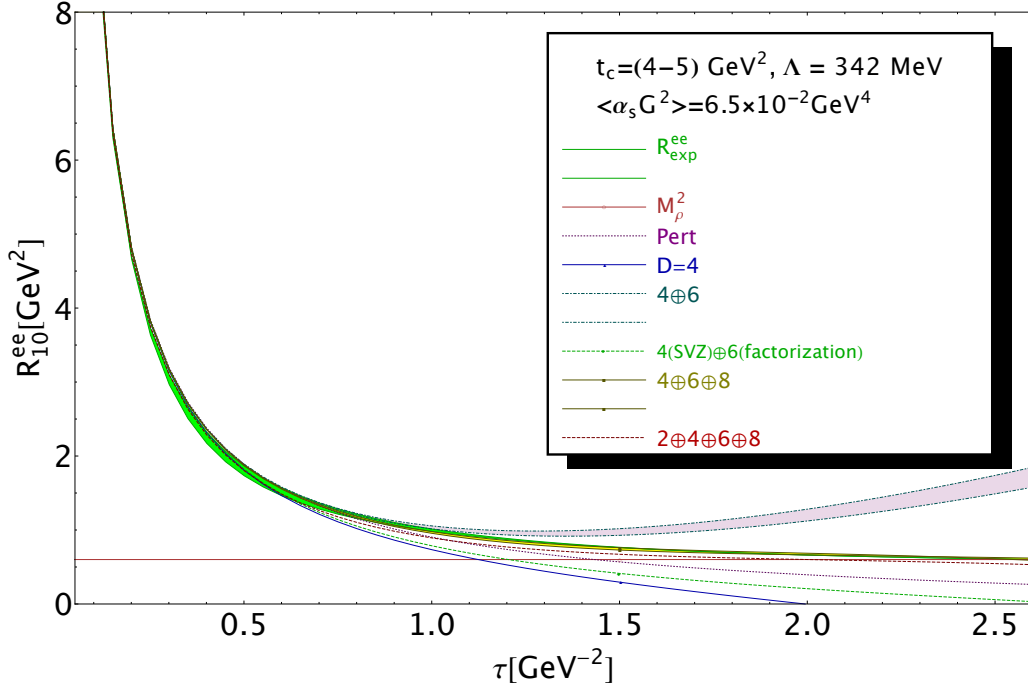


Figure 13:  $\tau$ -behaviour of the ratio of moments  $\mathcal{R}_{10}^{ee}$  for different truncation of the OPE.

– Combination of the standard value of the SVZ condensate and of factorization for the four-quark condensate gives a better agreement with the data here than in the case of the ratio of moments. However, as mentioned previously, a simultaneous use of these two values is (unfortunately) inconsistent with the fitted ones from different approaches.

## 8. $\alpha_s$ from the lowest $\tau$ -like decay moment

$\tau$ -like decay moments applied to  $e^+e^- \rightarrow \text{Hadrons}$  have been initially used in Refs. [35, 60] to extract  $\alpha_s$  and the QCD condensates. Using the previous values of the QCD non-perturbative (NP) parameters into the  $\tau$ -like decay rate (lowest moment) [54]:

$$R_\tau^{ee} = \int_0^1 dx_0 (1 - 3x_0^2 + 2x_0^3) 2R_{ee}^{I=1}(x_0) \quad (49)$$

with  $x_0 \equiv (t/M_0^2)$ , we attempt to extract the value of  $\alpha_s$  for different values of  $M_0$ .

### • The QCD expression of $R_\tau^{ee}$

We shall use its expression within Fixed Order perturbation theory (FO)<sup>5</sup>. In our analysis, we shall omit non-standard effects due to instantons and duality violation where the effects are expected to be negligible [36, 51]. Renormalon ones induced by the large  $\beta$  approximation of the higher order

<sup>5</sup>There are some recent attempts to reconcile FO and Contour Improved (CI) approach (see e.g. [61]).

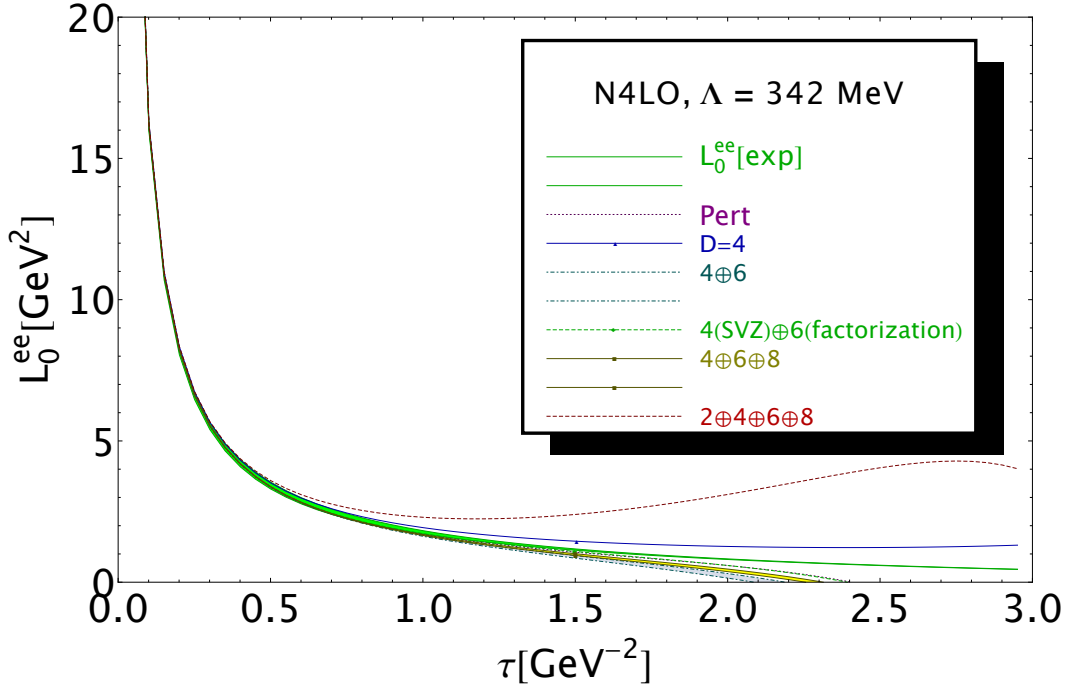


Figure 14:  $\tau$ -behaviour of the lowest moment  $\mathcal{L}_0$  for different truncation of the OPE.

terms of PT [62, 63] will not also be considered like its tachyonic gluon mass effects [4] and Padé approximants alternative. However, their eventual effects are expected to be smaller than the size of the errors in our analysis.

Following the notations of BNP, the QCD expression of the moment can be written as:

$$R_\tau^{ee}|_{qcd} = \frac{N_c}{2} \left[ 1 + \delta_{ee}^0 + \sum_{D=1,2,\dots} \delta_{ee}^{(2D)} \right]. \quad (50)$$

◊ The QCD expression copied from BNP [54] reads within FO perturbation theory in the  $\overline{MS}$  scheme :

$$\delta_{ee}^{(0)}|_{FO} = a_s + 5.2023 a_s^2 + 26.366 a_s^3 + 127.079 a_s^4, \quad (51)$$

where the last term comes from [27]. The power corrections read:

$$\begin{aligned} \delta_{ee}^{(2)} &= -12(1 + 4a_s) \frac{(m_u^2 + m_d^2)}{M_0^2}, & \delta_{ee}^{(2)}|_{tach} &= -2 \times 1.05 \frac{a_s \lambda^2}{M_0^2}, \\ \delta_{ee}^{(4)} &= \frac{11\pi}{4} a_s^2 \frac{\langle \alpha_s G^2 \rangle}{M_0^4} - \frac{2\pi^2 a_s^2}{M_0^4} \left[ 9 \langle m_u \bar{\psi}_u \psi_u + m_d \bar{\psi}_d \psi_d \rangle + 4 \sum_k \langle m_k \bar{\psi}_k \psi_k \rangle \right] + 36 \frac{(m_u^4 + m_d^4)}{M_0^4}, \\ \delta_{ee}^{(6)} &= -6 \frac{d_6}{M_0^6}, & \delta_{ee}^{(8)} &= -4 \frac{d_8}{M_0^8}, \end{aligned} \quad (52)$$

where  $d_6$  and  $d_8$  have been defined in Eqs. 15 and 16. We have shown the  $D = 2$  contribution due to an eventual tachyonic gluon mass not included in the standard OPE.

◊ Using the Contour Improved (CI) approach, the QCD PT series read [27, 52]:

$$\delta_{ee}^{(0)}|_{CI} = 1.364 a_s + 2.54 a_s^2 + 9.71 a_s^3 + 64.29 a_s^4, \quad (53)$$

◊ Assuming that the PT series grow geometrically [29] as observed from the calculated coefficients, we estimate the  $a_s^5$  coefficient to be :

$$p_5^{FO} \approx +597, \quad p_5^{CI} \approx +426, \quad (54)$$

which we consider either to be the error due to the higher order terms of the series or (more optimistically) to be the estimate of the uncalculated  $\alpha_s^5$  coefficient. A check of the sign and size of this estimate from another approach is welcome to test if the PT series already reach its asymptotic at this order and if the large  $\beta$ -approach is a good approximation.

• *Numerical analysis*

◊ We insert into  $R_\tau^{ee}|_{qcd}$  the value of the condensates given in Eqs. 11 and 37. We extract  $\alpha_s$  for different values of  $M_0$  using the Mathematica Program NSolve. Next we run each result to  $M_\tau$  using the evolution equation:

$$a_s(M_\tau) = a_s(M_0) \left\{ 1 + a_s(M_0) \log(x_0) \left[ \frac{\beta_1}{2} + a_s(M_0) \left( \frac{\beta_2}{2} + \frac{\beta_1^2}{4} \log(x_0) \right) \right] \right\} + \mathcal{O}(a_s^4) \quad (55)$$

◊ We show the different values of  $a_s(M_\tau)$  extracted at each value of  $M_0$  in Fig. 15. We notice a nice stability of the results versus  $M_0$  in the range 1.45 to 1.7 GeV. We obtain to  $\mathcal{O}(\alpha_s^4)$ :

$$\begin{aligned} \alpha_s^{FO}(M_\tau) &= 0.3247(46)_{fit(1)_{np}(62)_{h.o}} = 0.3247(77) \rightarrow \alpha_s^{FO}(M_Z) = 0.1191(10)(3) \\ \alpha_s^{CI}(M_\tau) &= 0.3483(63)_{fit(1)_{np}(15)_{h.o}} = 0.3483(65) \rightarrow \alpha_s^{CI}(M_Z) = 0.1218(8)(3), \end{aligned} \quad (56)$$

where the dominant error comes from the fitting procedure and the estimate of the higher order corrections. The last error in  $\alpha_s(M_Z)$  comes from the running procedure. We deduce the mean :

$$\alpha_s(M_\tau) = 0.3385(50)(136)_{syst} \rightarrow \alpha_s(M_Z) = 0.1207(17)(3), \quad (57)$$

where  $\pm 136$  is an added conservative systematic from the distance of the mean to the FO/CI central values.  $\pm 3$  is an error induced by the running procedure.

◊ The error due to the non-perturbative (n.p) terms are negligible for FO and CI.

◊ We have not included the effects beyond the standard OPE (tachyonic gluon, instantons, duality violation) in our analysis which have been estimated to be small [35]. The previous values of  $\alpha_s(M_\tau)$  are in agreement, within the errors, with some other determinations from  $V/A/V+A$  hadronic  $\tau$ -decay data for FO and CI within the standard OPE (see Table 2).

◊ We have not included in Table 2 some analysis including a duality violation [46, 51] and PT  $\oplus$  renormalon [62, 63] which leads to smaller values of  $\alpha_s(M_\tau)$ . The mean of different FO/CI determinations up to  $\mathcal{O}(\alpha_s^4)$  in Table 2 is :

$$\langle \alpha_s(M_\tau) \rangle = 0.3336(31)(116)_{syst} \rightarrow \langle \alpha_s(M_Z) \rangle = 0.1201(14)(3). \quad (58)$$

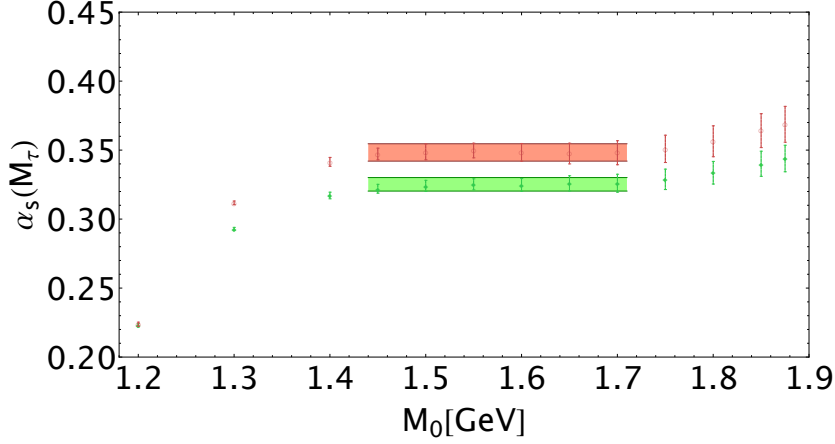


Figure 15: Value of  $\alpha_s(M_\tau)$  to  $\mathcal{O}(\alpha_s^4)$  as a function of the hypothetical  $\tau$ -mass  $M_0$  including  $D \leq 8$  condensates. Green : FO. Red : CI. The errors due to the non-perturbative condensates and to the fitting procedure are shown.

◊ We notice that the size of the previously estimated higher order term (h.o) for FO is about the same as coming from renormalon or Padé approximants [62, 63]. Taken literally, the estimated  $\alpha_s^5$  coefficients in Eq. 54, the value of  $\alpha_s$  becomes to  $\mathcal{O}(\alpha_s^5)$ :

$$\begin{aligned} \alpha_s^{FO}(M_\tau)|_{+h.o} &= 0.3185(46) \quad \rightarrow \quad \alpha_s^{FO}(M_Z) = 0.1184(9) \\ \alpha_s^{CI}(M_\tau)|_{+h.o} &= 0.3401(61) \quad \rightarrow \quad \alpha_s^{CI}(M_Z) = 0.1209(7), \end{aligned} \quad (59)$$

which gives the mean:

$$\alpha_s(M_\tau) = 0.3263(37)(78)_{syst} = 0.3263(86) \quad \rightarrow \quad \alpha_s(M_Z) = 0.1193(11)(3) \quad (60)$$

## 9. Power corrections to the lowest $\tau$ -decay moment $R_\tau^{ee}$

### • $d_6$ from a one-parameter fit

To give a stronger constraint on  $d_6$ , we shall work with a one-parameter fit. We shall use as input the value of the gluon condensate in Eq. 11 and the previously determined values of  $\alpha_s(M_\tau)$  from  $R_\tau^{ee}$  in Eq. 56 and of  $d_8$  in Eq. 37 from  $\mathcal{R}_{10}$ . The result of the analysis is shown in Fig. 16 where one remarks that the result increases softly with the value of  $M_0$  and shows an almost stability (inflection point) around (1.8-1.9) GeV which is:

$$d_6 \simeq -(20 \sim 21) \times 10^{-2} \text{ GeV}^6 \quad (61)$$

with a 10% error. This result is identical to the one in Eq. 37. However, the results obtained from some other  $\tau$ -decay moments are also recovered in the  $M_0$ -instability region. We conclude that the extraction of  $d_6$  from the low  $\tau$ -decay moment is less accurate than the one from  $R_{10}^{ee}$ . It only gives an approximate range of values.

$\alpha_s^{FO}(M_\tau)$	$\alpha_s^{CI}(M_\tau)$	$\delta_{NP}^V(M_\tau) \times 10^{-2}$	Data	Refs.
<b>0.3247(77)</b>	<b>0.3483(65)</b>	<b><math>2.30 \pm 0.20</math></b>	$e^+e^-$	<b>This work</b>
0.350(50)	–	$1.45 \pm 1.3$	–	[60]
0.320(30)	–	$3.60 \pm 1.64$	$e^+e^- \oplus V+A : \tau\text{-decay}$	[35]
0.320(22)	0.340(23)	$2.0 \pm 1.7$	$V : \tau\text{-decay}$	ALEPH [47]
0.323(16)	0.347(23)	$1.87 \pm 0.54$	$V : \tau\text{-decay}$	OPAL [48]
0.328(9)	–	–	$V+A : \tau\text{-decay}$	[36]
0.322(16)	0.342(16)	–	$V+A : \tau\text{-decay}$	[27]
0.324(11) <sup>*</sup>	0.346(11)	–	$V+A : \tau\text{-decay}$	ALEPH [50]
0.320(12)	0.335(13)	–	$V+A : \tau\text{-decay}$	[51]
<i>0.3243(42)</i>	<i>0.3452(47)</i>	<i><math>2.28 \pm 0.20</math></i>		<i>Mean</i>

Table 2:  $\alpha_s(M_\tau)$  and  $\delta_{NP}^V$  from  $\tau$ -decay moments within fixed order (FO) and contour improved (CI) perturbative series up to  $\mathcal{O}(\alpha_s^4)$ . <sup>\*</sup>) indicates that the quoted error is our crude estimate.

• *Sum of power corrections to the lowest  $\tau$ -decay moment  $R_\tau^{ee}$*

◊ Using our previous determinations of the condensates, we can estimate the sum of the power corrections to  $R_\tau^{ee}$ . In so doing, we introduce as input the value of  $\alpha_s(M_\tau)$  determined previously and the value of the gluon condensate in Eq. 11. To minimize the number of free parameters, we first neglect the contribution of high-dimension condensates  $D \geq 10$  and assume that the retained condensate  $D = 8$  is an effective condensate which absorbs into it all unknown high-dimension condensate effects.

◊ Then, using the values of  $d_4$  in Eq.11,  $d_6$  and  $d_8$  in Eq.37, we deduce the sum of the NP contributions :

$$\delta_{NP}^V(M_\tau) = (2.3 \pm 0.2) \times 10^{-2}, \quad (62)$$

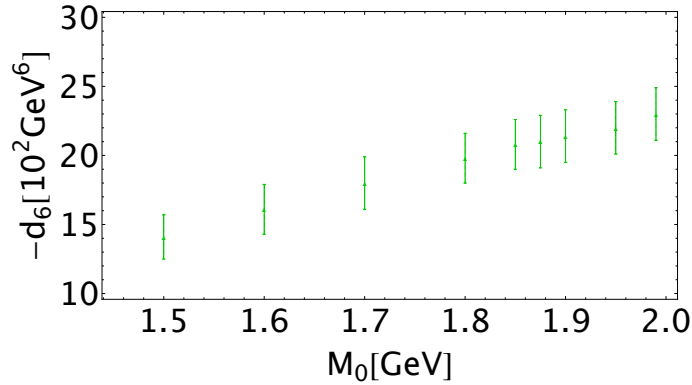


Figure 16:  $d_6$  condensate as function of the hypothetical  $\tau$ -mass  $M_0$  using  $\alpha_s(M_0)$ ,  $d_4$  and  $d_8$  from  $\mathcal{R}_{10}$  as inputs.

which improves our previous findings from  $e^+e^- \rightarrow I = 1$  hadrons data:  $\delta_{NP}^V(M_\tau) = (2.38 \pm 0.89) \times 10^{-2}$  in Ref. [35] and the analysis in [36].

◊ It is remarkable to notice that this value agrees with the one from  $\tau$ -decay analysis (see Table 2) despite the large discrepancies with the individual values of each condensate. This is due to the alternate signs of the condensate contributions in the  $\tau$ -moments.

◊ One can also notice that the value of  $\alpha_s$  decreases with the  $\delta_{NP}$ . From  $\delta_{NP}^V = 3.7 \times 10^{-2}$  (our first iteration in Eq. 32) to the final value:  $2.3 \times 10^{-2}$  (Eqs. 37 and 38), the value of  $\alpha_s(M_\tau)$  moves slightly from 0.329 to 0.325.

## 10. $a_\mu|_{l.o}^{hvp}$ from $e^+e^- \rightarrow$ hadrons data

We complete the analysis by updating our previous determination of the lowest order hadronic contributions to the vacuum polarization of  $a_\mu$  [19]. This analysis will also serve as a test of our parametrization of the  $I = 1$  part of the spectral function used in previous sections.

The lowest order hadronic contributions to the vacuum polarization can be obtained from the well-known dispersion relation [64–68]:

$$a_\mu \equiv \frac{1}{2}(g - 2)_\mu = \frac{1}{4\pi^3} \int_{4m_\pi^2}^{\infty} dt K_\mu(t) \sigma(e^+e^- \rightarrow \text{hadrons}) \quad (63)$$

where  $K_\mu(t)$  is the QED kernel function [69]:

$$K_\mu(t) = \int_0^1 dx \frac{x^2(1-x)}{x^2 + (t/m_\mu^2)(1-x)}. \quad (64)$$

- $a_\mu|_{l.o}^{hvp}$  from  $e^+e^- \rightarrow I = 1$  hadrons below 1.875 GeV and test of our parametrization

This analysis is an update of the one in Ref. [19] and will also serve as a test of our parametrization of the data especially for the  $\rho$ -meson where we have only used a minimal Breit-Wigner for the pion form factor. We obtain the contributions given in Table 3 for the three subdivision regions of the data below 1.875 GeV as shown in Figs. 1, 2 and 3.

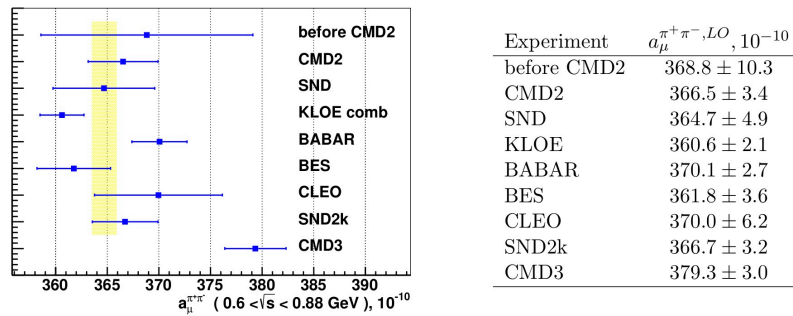


Figure 17: Comparison of the  $\rho$ -meson contribution to  $a_\mu$  for  $0.6 \leq \sqrt{s} \leq 0.88$  GeV from [44].

$\sqrt{t}[\text{GeV}]$	$a_\mu _{l.o}^{hvp} \times 10^{11}$	$a_\tau _{l.o}^{hvp} \times 10^9$	$\Delta\alpha_{had}^{(5)}(M_Z^2) \times 10^5$
<b>Light I=1</b>			
$\rho(2m_\pi \rightarrow 0.50)$	$489.4 \pm 3.1$	$85.1 \pm 0.6$	$12.38 \pm 0.08$
$\rho(0.50 \rightarrow 0.60)$	$524.5 \pm 13.7$	$135.9 \pm 3.5$	$22.84 \pm 0.59$
$\rho(0.60 \rightarrow 0.776)$	$2712.0 \pm 30.2$	$943.7 \pm 10.3$	$182.87 \pm 1.97$
$\rho(0.776 \rightarrow 0.993)$	$1297.3 \pm 9.8$	$1797.3 \pm 20.3$	$117.82 \pm 0.98$
$0.993 \rightarrow 1.5$	$354.4 \pm 6.7$	$228.2 \pm 4.1$	$67.3 \pm 1.14$
$1.5 \rightarrow 1.875$	$237.6 \pm 5.7$	$206.8 \pm 4.9$	$80.11 \pm 1.9$
<i>Total Light I=1 (<math>\leq 1.875</math>)</i>	<i><math>5615.2 \pm 36.0</math></i>	<i><math>2453.3 \pm 11.9</math></i>	<i><math>483.3 \pm 4.4</math></i>
<b>Light I=0</b>			
$\omega$ (NWA)	$417.1 \pm 13.7$	$163.3 \pm 5.3$	$33.6 \pm 1.1$
$\phi$ (NWA)	$389.6 \pm 4.6$	$20.6 \pm 0.2$	$51.2 \pm 0.6$
$0.993 \rightarrow 1.5$	$44.3 \pm 0.8$	$28.5 \pm 0.5$	$8.4 \pm 0.1$
$\omega(1650)(\text{BW})$	$24.3 \pm 0.1$	$16.7 \pm 0.1$	$5.2 \pm 0.1$
$\phi(1680)(\text{BW})$	$1.8 \pm 0.9$	$1.3 \pm 0.6$	$0.4 \pm 0.2$
<i>Total Light I=0 (<math>\leq 1.875</math>)</i>	<i><math>877.1 \pm 14.5</math></i>	<i><math>230.4 \pm 5.3</math></i>	<i><math>99.4 \pm 1.3</math></i>
<b>Light I=0 <math>\oplus</math> 1</b>			
$1.875 \rightarrow 1.913$	$14.7 \pm 0.7$	$14.4 \pm 0.7$	$6.3 \pm 0.3$
$1.913 \rightarrow 1.96$	$17.6 \pm 0.6$	$17.5 \pm 0.6$	$7.9 \pm 0.3$
$1.96 \rightarrow 2$	$14.3 \pm 0.5$	$14.5 \pm 0.5$	$6.7 \pm 0.2$
$2 \rightarrow 3.68$ : QCD ( $u, d, s$ )	$247.2 \pm 0.3$	$308.3 \pm 0.5$	$202.8 \pm 0.5$
<i>Total Light I=0 <math>\oplus</math> 1 (<math>1.875 \rightarrow 3.68</math>)</i>	<i><math>293.8 \pm 1.1</math></i>	<i><math>354.7 \pm 1.2</math></i>	<i><math>223.7 \pm 0.7</math></i>
<b>Total Light I=0 <math>\oplus</math> 1 (<math>2m_\pi \rightarrow 3.68</math>)</b>	<b><math>6786.1 \pm 38.8</math></b>	<b><math>3038.4 \pm 24.5</math></b>	<b><math>806.4 \pm 4.6</math></b>
<b>Charmonium</b>			
$J/\psi(1S)$ (NWA)	$65.1 \pm 1.2$	$92.7 \pm 1.8$	$73.5 \pm 1.4$
$\psi(2S)$ (NWA)	$16.4 \pm 0.6$	$26.0 \pm 0.9$	$26.1 \pm 0.8$
$\psi(3773)$ (NWA)	$1.7 \pm 0.1$	$2.7 \pm 0.2$	$2.9 \pm 0.2$
<i>Total <math>J/\psi(\text{NWA})</math></i>	<i><math>83.2 \pm 1.4</math></i>	<i><math>121.4 \pm 2.0</math></i>	<i><math>102.5 \pm 1.6</math></i>
$3.69 \rightarrow 3.86$	$11.4 \pm 1.0$	$18.3 \pm 1.6$	$19.0 \pm 1.6$
$3.86 \rightarrow 4.094$	$16.6 \pm 0.5$	$27.5 \pm 0.8$	$30.9 \pm 0.9$
$4.094 \rightarrow 4.18$	$6.6 \pm 0.2$	$11.2 \pm 0.3$	$13.2 \pm 0.4$
$4.18 \rightarrow 4.292$	$6.5 \pm 0.2$	$11.2 \pm 0.4$	$13.7 \pm 0.5$
$4.292 \rightarrow 4.54$	$11.8 \pm 0.6$	$20.7 \pm 0.8$	$26.8 \pm 1.1$
$4.54 \rightarrow 10.50$ : QCD ( $u, d, s, c$ )	$92.0 \pm 0.0$	$186.2 \pm 0.0$	$458.73 \pm 0.1$
<i>Total Charmonium (<math>3.69 \rightarrow 10.50</math>)</i>	<i><math>145.1 \pm 1.3</math></i>	<i><math>275.6 \pm 2.0</math></i>	<i><math>564.9 \pm 2.2</math></i>
<b>Total Charmonium</b>	<b><math>228.1 \pm 1.9</math></b>	<b><math>396.5 \pm 2.8</math></b>	<b><math>664.8 \pm 2.7</math></b>
<b>Bottomium</b>			
$\Upsilon(1S)$ (NWA)	$0.54 \pm 0.02$	$1.25 \pm 0.07$	$5.65 \pm 0.29$
$\Upsilon(2S)$ (NWA)	$0.22 \pm 0.02$	$0.51 \pm 0.06$	$2.54 \pm 0.29$
$\Upsilon(3S)$ (NWA)	$0.14 \pm 0.02$	$0.33 \pm 0.04$	$1.77 \pm 0.23$
$\Upsilon(4S)$ (NWA)	$0.10 \pm 0.01$	$0.23 \pm 0.03$	$1.26 \pm 0.16$
$\Upsilon(10.86 \oplus 11)$ (NWA)	$0.1 \pm 0.06$	$0.20 \pm 0.06$	$1.67 \pm 0.39$
<i>Total Bottomium (NWA)</i>	<i><math>1.0 \pm 0.1</math></i>	<i><math>2.3 \pm 0.1</math></i>	<i><math>11.2 \pm 0.5</math></i>
$Z - \text{pole}$	-	-	$29.2 [81]$
$10.59 \rightarrow 2m_t$ : QCD ( $u, d, s, c, b$ )	$22.4 \pm 0.3$	$57.5 \pm 0.1$	$1282.9 \pm 1.2$
<b>Total Bottomium</b>	<b><math>23.4 \pm 0.3</math></b>	<b><math>59.8 \pm 0.1</math></b>	<b><math>1323.3 \pm 1.3</math></b>
$2m_t \rightarrow \infty$ : QCD ( $u, d, s, c, b, t$ )	0.03	0.08	-28.2
<b>Total sum</b>	<b><math>7036.5 \pm 38.9</math></b>	<b><math>3494.8 \pm 24.7</math></b>	<b><math>2766.3 \pm 4.5</math></b>

Table 3:  $a_\tau|_{l.o}^{hvp}$ ,  $a_\mu|_{l.o}^{hvp}$  and  $\alpha(M_Z^2)$  within our parametrization of the compiled PDG [43]  $\oplus$  the recent CMD3 [44].



◇ *Comparison with some other determinations for  $0.60 \leq \sqrt{t} \leq 0.88$  GeV*

We compare our determinations from the  $\rho$ -meson using a minimal Breit-Wigner parametrization of the pion form factor for  $0.6 \leq \sqrt{t} \leq 0.88$  GeV :

$$a_\mu^\rho|_{l.o}^{hvp}[0.6 \rightarrow 0.88] = (370.5 \pm 2.1) \times 10^{-10}. \quad (65)$$

Despite our minimal parametrization of the pion form factor, our result is in a good agreement with the previous ones in Fig.17 using a more involved parametrization. We interpret our slightly lower value compared to CMD3 [44] from the fact that the minimal fit cannot accommodate accurately the data in this region.

◇ *Improving the  $\rho$  meson contribution below 0.993 GeV*

Though our minimal BW parametrization is in agreement with previous determination given in Fig. 17, we can see in Fig. 1 that there are regions which need to be improved. This is necessary for the high-precision determination of  $a_\mu$ . Notice that, within the modest accuracy of the results in previous sections, this improvement only affects slightly these results. In so doing , we subdivide the region below 0.993 GeV into 6 subregions in units of GeV :

$$[2m_\pi \rightarrow 0.5], [0.5 \rightarrow 0.6], [0.6 \rightarrow 0.776], [0.776 \rightarrow 0.786], [0.786 \rightarrow 0.810], [0.810 \rightarrow .993]. \quad (66)$$

We use the tail of the Breit-Wigner for  $[2m_\pi \rightarrow 0.5]$  as shown in Fig. 1 and different polynomials within the FindFit Mathematica program with optimised  $\chi^2$  to fit the other regions from  $0.5 \rightarrow .993$  GeV. We remind that the new CMD3 data [44] are 2-3 times more precise than the one compiled by PDG[43] but the central values are approximately similar except in the low energy region where the CMD3 data are slightly higher. We show the analysis in Figs. 18 and 19. Notice that, in the region 0.776 to 0.86 GeV, we have only considered the data from CMD3 (red). The effect of this region to  $a_\mu$  from CMD3 data is  $(206.5 \pm 1.7) \times 10^{-11}$  while the one using the BW in Fig.1 gives  $(205.7 \pm 1.03) \times 10^{-11}$  such that the difference by using the two data is negligible. The different contributions are given in Table 3. From the fit improvement the result in Eq. 65 becomes :

$$a_\mu^\rho|_{l.o}^{hvp}[0.6 \rightarrow 0.88] = (377.4 \pm 3.1) \times 10^{-10}. \quad (67)$$

It is also informative to give our result in the so-called intermediate region  $[0.6 \rightarrow 0.993]$  GeV:

$$a_\mu^\rho|_{l.o}^{hvp}[0.6 \rightarrow 0.993] = (400.9 \pm 3.2) \times 10^{-10}. \quad (68)$$

◇  *$a_\mu^{I=1}|_{l.o}^{hvp}$  from .993 to 1.875 GeV*

The fits of these regions have been done in previous sections. The result is given in Table 3.

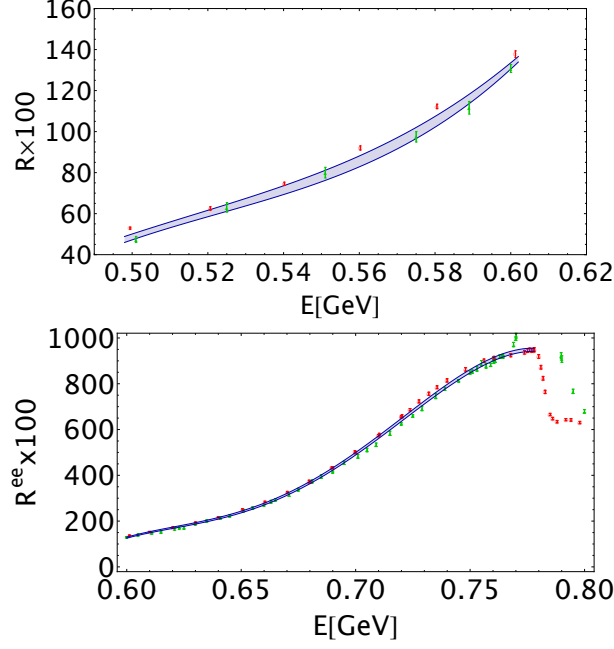


Figure 18: Fit of the data in the region 0.5 to 0.776 GeV.

- $a_\mu$  from  $e^+e^- \rightarrow I = 0$  hadrons below 1.875 GeV

◊  $\omega$  and  $\phi$  mesons contributions

We estimate the  $\omega$  and  $\phi$  mesons contribution using a narrow width approximation (NWA). It reads [19]:

$$a_\mu^{I=0}|_{l.o}^{hvp} = \frac{3}{\pi} \sum_{R=\omega,\phi} \frac{\Gamma_R^{ee}}{M_R} K_\mu(M_R^2). \quad (69)$$

Using [43] :

$$\begin{aligned} \Gamma_\omega^{ee} &= (64 \pm 1.9 \pm 0.96) \times 10^{-2} \text{ keV}, & \Gamma_\phi^{ee} &= (126.6 \pm 1.4 \pm 0.4) \times 10^{-2} \text{ keV} \\ M_\omega &= (782.66 \pm 0.13) \text{ MeV}, & M_\phi &= (1019.461 \pm 0.016) \text{ MeV}, \end{aligned} \quad (70)$$

the result is given in Table 3.

◊  $a_\mu^{I=0}|_{l.o}^{hvp}$  from .993 to 1.5 GeV

We add the  $I = 0$  contribution subtracted for the  $I = 1$  analysis in the previous sections by using the  $SU(3)$  relation. We obtain the value in Table 3.

◊  $a_\mu^{I=0}|_{l.o}^{hvp}$  from 1.5 to 1.875 GeV

We consider the contributions of the  $\omega(1650)$  and  $\phi(1680)$ . We use the parameters deuced from PDG22 [43]:

$$\begin{aligned} \omega(1650) &: M_\omega = (1670 \pm 30) \text{ MeV}, & \Gamma_\omega^{ee} &= 1.35 \pm 0.14 \text{ keV}, & \Gamma_\omega^h &= 315 \pm 35 \text{ MeV} \\ \phi(1680) &: M_\phi = (1680 \pm 20) \text{ MeV}, & \Gamma_\phi^{ee} &= 0.18 \pm 0.06 \text{ keV}, & \Gamma_\phi^h &= 150 \pm 50 \text{ MeV}. \end{aligned} \quad (71)$$

Using a Breit-Wigner (BW) parametrization, we obtain the value in Table 3.

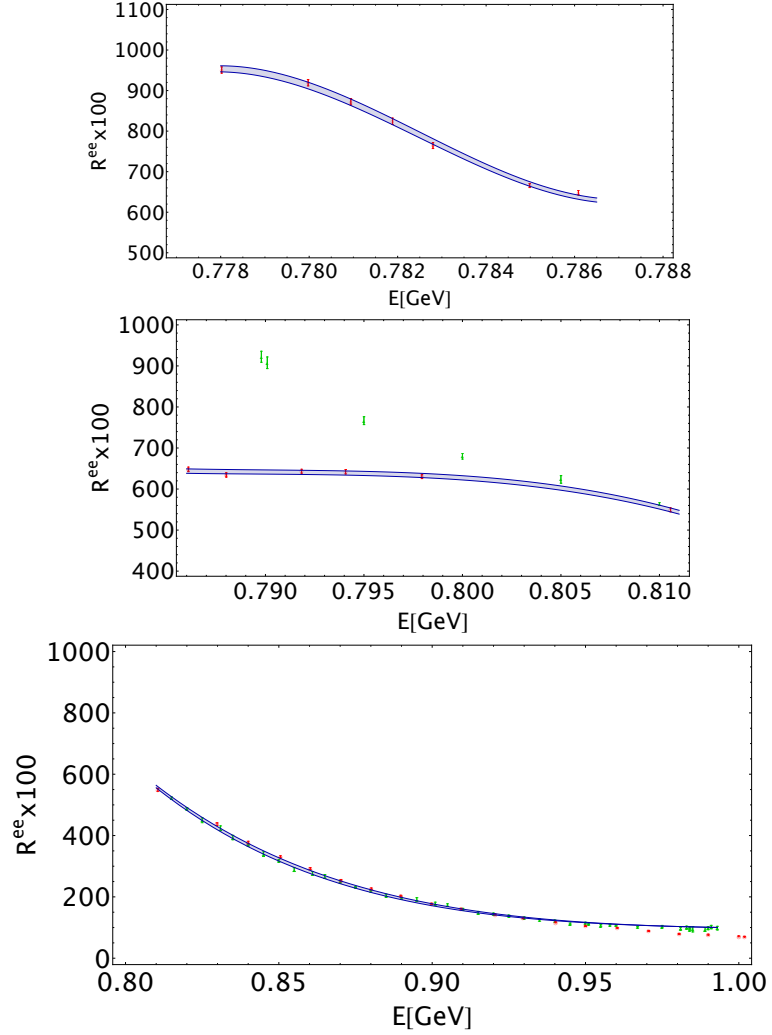


Figure 19: Fit of the data in the region 0.776 to 0.993 GeV.

- $a_\mu|_{l.o}^{hvp}$  from 1.875 to 2 GeV

To get this contribution, we divide the data into three regions and fit with polynomials using the optimized  $\chi^2$  Mathematica program FindFit. The fits of the data are shown in Fig.20.

- $a_\mu|_{l.o}^{hvp}$  from 2 to 3.68 GeV

The data in this region are well fitted by the QCD expression of the spectral function for 3 flavours as one can see from Fig. 21 given by PDG. To the massless PT expression known to order  $\alpha_s^4$ , we include the quark and gluon condensates of dimensions  $D = 4, 6$  (see Eqs.4 to 15). We add the quadratic  $m_s^2$ -corrections to order  $\alpha_s^3$  and the quartic  $m_s^4$ -mass corrections to order  $\alpha_s^2$  [70]. These quark mass corrections read in the  $\overline{MS}$ -scheme:

$$\begin{aligned}
 d_{2m} &= -\frac{\overline{m}_s^2}{t} (12 a_s + 104.833 a_s^2 + 541.735 a_s^3), \\
 d_{4m} &= \frac{\overline{m}_s^4}{t^2} \left[ -6(1 + \frac{11}{3} a_s) + a_s^2 \left[ n_f \left( \frac{L_m}{3} - 1.841 \right) - \frac{11}{2} L_m + 136.693 + 12 - 0.475 - L_m \right] \right] \quad (72)
 \end{aligned}$$

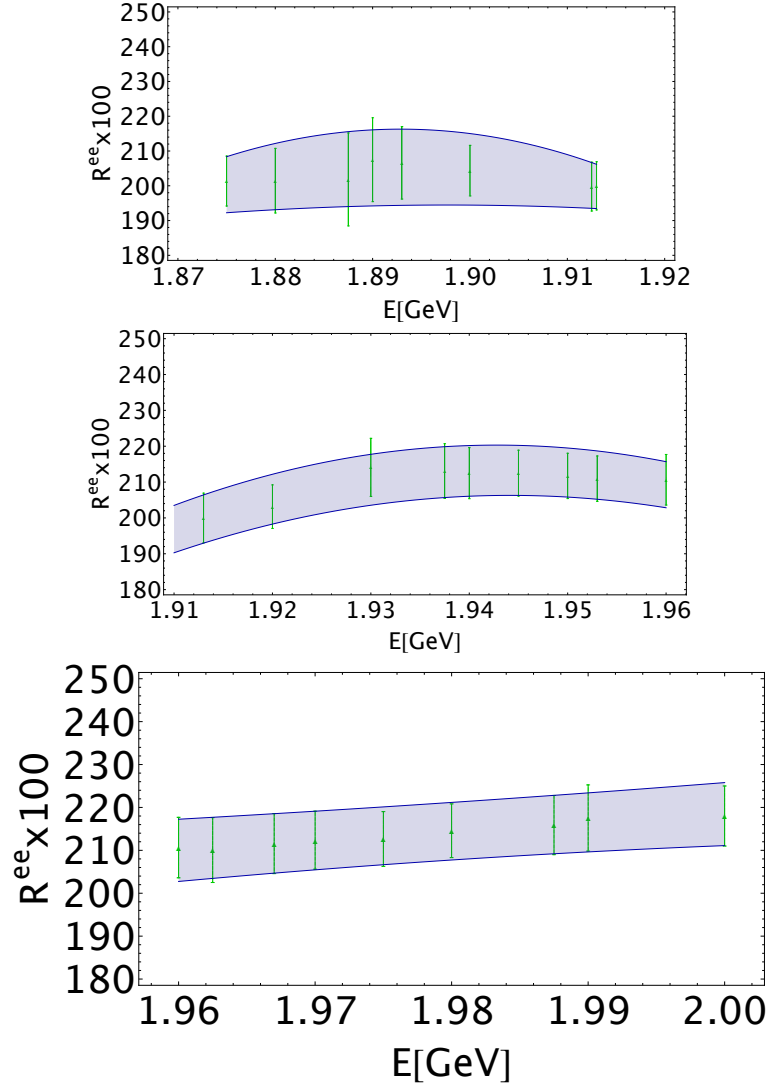


Figure 20: Fit of the data in the region 1.875 to 2 GeV.

where  $\overline{m}$  is the running quark mass and  $L_m \equiv \text{Log}(\overline{m}_s^2/t)$ . In the numerical analysis, we shall also introduce the RGI quark mass defined as [71]:

$$\overline{m}_s(\nu) = \hat{m}_s (-\beta_1 a_s(\nu))^{-\gamma_1 \beta_1} [1 + \mathcal{O}(a_s)], \quad (73)$$

where  $\gamma_1 = 2$  is the quark mass anomalous dimension and  $\beta_1 = -(11 - 2n_f/3)/2$  the first coefficient of the  $\beta$ -function. The expression to order  $a_s^2$  which we shall use can be found e.g. in Ref. [6]. We shall use  $\hat{m}_s = 116(6)$  MeV [7].

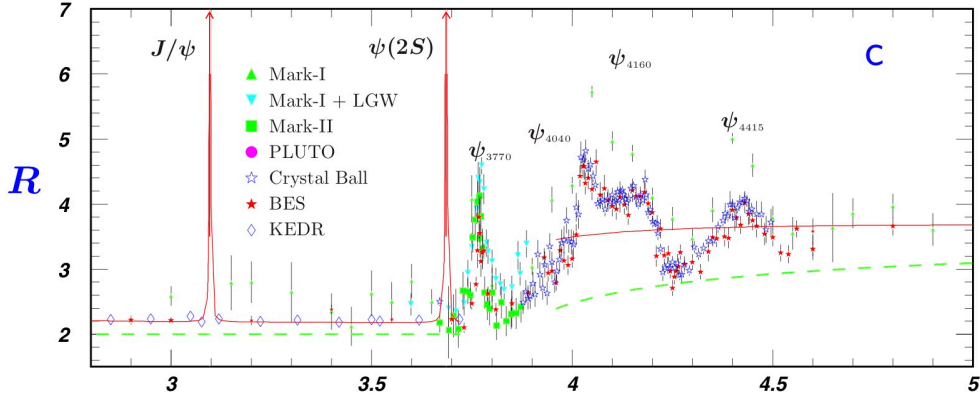


Figure 21:  $e^+e^- \rightarrow \text{Hadrons}$  data in the charmonium region from 2 to 5 GeV from PDG [43].

•  $a_\mu|_{l.o}^{hvp}$  from charmonium

◊ The  $J/\psi(1S), \psi(2S)$  and  $\psi(3773)$  contributions

We estimate their contributions using a NWA and the values of the masses and widths from PDG [43]:

$$\begin{aligned}
 \psi(1S) &: M_\psi = (3069.9 \pm 0.006) \text{ MeV}, & \Gamma_\psi^{ee} &= (5.53 \pm 0.10) \text{ keV}, & \Gamma_\psi^h &= (92.6 \pm 1.0) \text{ keV}. \\
 \psi(2S) &: M_\psi = (3681.1 \pm 0.06) \text{ MeV}, & \Gamma_\psi^{ee} &= (2.33 \pm 0.08) \text{ keV}, & \Gamma_\psi^h &= (294 \pm 8) \text{ keV}. \\
 \psi(3773) &: M_\psi = (3773.7 \pm 0.4) \text{ MeV}, & \Gamma_\psi^{ee} &= (0.26 \pm 0.02) \text{ keV}, & \Gamma_\psi^h &= (27.2 \pm 1.0) \text{ MeV}.
 \end{aligned}$$

The result is given in Table 3.

◊ Region from 3.68 to 4.55 GeV

We divide this region into 5 subregions as shown in Fig. 22. The region between 3.68 to 3.86 is better fitted using a Breit-Wigner while in the others, we use polynomials. The different contributions are shown in Table 3.

◊ Region from 4.55 to 10.50 GeV

As shown in Figs. 21 and 23, the data without resonance peaks are well fitted by QCD for 4 flavours. We add to the previous QCD expressions the charm contributions with  $m_c^2$  and  $m_c^4$  mass corrections where  $\overline{m}_c(\overline{m}_c) = 1266(6) \text{ MeV}$  [7]. The contribution is given in Table 3.

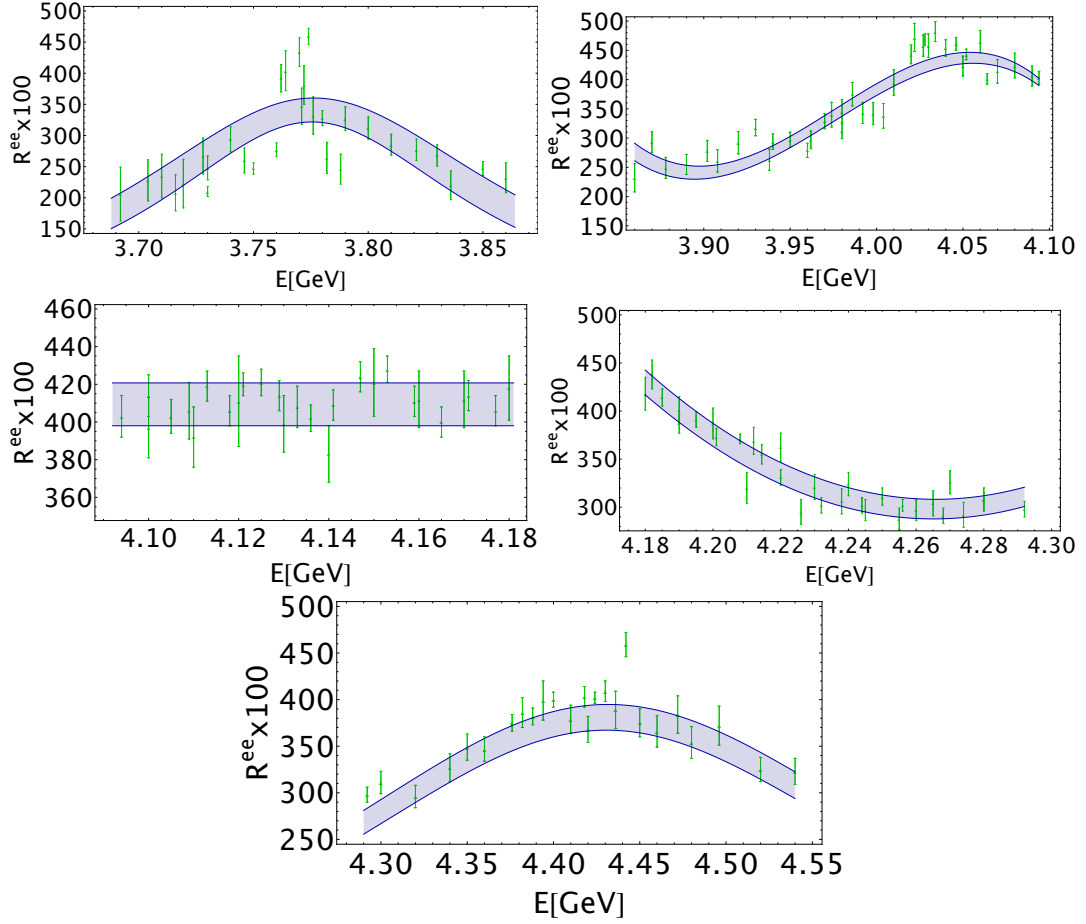


Figure 22: Fits of the  $e^+e^- \rightarrow \text{Hadrons}$  data in the charmonium region from 3.68 to 4.55 GeV from PDG [43].

•  $a_\mu|_{l.o}^{hvp}$  from bottomium

◊  $\Upsilon(1S \rightarrow 11.02)$  contributions

We use a NWA to estimate their contributions with:

$$\begin{aligned}
 \Upsilon(1S) &: M_\Upsilon = (9460.30 \pm 0.26) \text{ MeV}, & \Gamma_\Upsilon^{ee} &= (1.286 \pm 0.067) \text{ keV}, & \Gamma_\Upsilon^h &= (954.02 \pm 1.25) \text{ keV}, \\
 \Upsilon(2S) &: M_\Upsilon = (10023.26 \pm 0.31) \text{ MeV}, & \Gamma_\Upsilon^{ee} &= (0.611 \pm 0.071) \text{ keV}, & \Gamma_\Upsilon^h &= (31.98 \pm 2.63) \text{ keV}, \\
 \Upsilon(3S) &: M_\Upsilon = (10355.2 \pm 0.5) \text{ MeV}, & \Gamma_\Upsilon^{ee} &= (0.443 \pm 0.057) \text{ keV}, & \Gamma_\Upsilon^h &= (20.32 \pm 1.85) \text{ keV}, \\
 \Upsilon(4S) &: M_\Upsilon = (10579.4 \pm 1.2) \text{ MeV}, & \Gamma_\Upsilon^{ee} &= (0.322 \pm 0.042) \text{ keV}, & \Gamma_\Upsilon^h &= (20.5 \pm 2.5) \text{ keV}. \quad (75)
 \end{aligned}$$

◊  $QCD$  continuum contribution from 10.59 GeV to  $2m_t$

We add the  $b$ -quark contribution to the previous  $QCD$  expression where  $b$ -quark mass corrections to order  $a_s^3 \overline{m}_b^2/t$  and  $a_s^2 \overline{m}_b^4/t^2$  are included. We use  $\overline{m}_b(\overline{m}_b) = 4202(8) \text{ MeV}$  [7]. For the analysis, we consider the region from 10.59 MeV to  $2m_t$  just after the  $\Upsilon(4S)$  where the  $QCD$  continuum is

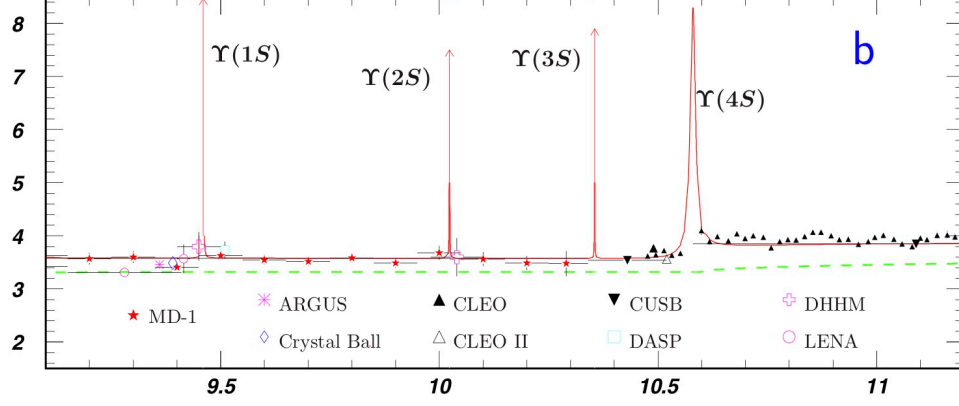


Figure 23:  $e^+e^- \rightarrow \text{Hadrons}$  data in the bottomonium region from 9 to 10.5 GeV from PDG [43].

expected to smear the  $\Upsilon(10860, 11020)$  and some eventual higher resonances. The result is given in Table 3.

◇ *QCD continuum contribution from  $2m_t \rightarrow \infty$*

Due to the heaviness of the top quark mass, we shall use the approximate Schwinger formula near the  $\bar{t}t$  threshold for a much better description of the spectral function up to order  $\alpha_s$  due to the top quark:

$$R_t^{ee} = \frac{4}{3}v \frac{(3-v^2)}{2} \left[ 1 + \frac{4}{3}\alpha_s f(v) \right], \quad (76)$$

with:

$$f(v) = \frac{\pi}{2v} - \frac{(3+v)}{4} \left( \frac{\pi}{2} - \frac{3}{4\pi} \right) : \quad v = \left( 1 - \frac{m_t^2}{t} \right)^{1/2}. \quad (77)$$

Here  $m_t$  is the on-shell top quark mass which we fix to be [43]<sup>6</sup>:

$$\bar{m}_t(\bar{m}_t^2) = (172.7 \pm 0.3) \text{ GeV}, \quad (78)$$

from some direct measurements. We add to this expression the one due to  $\alpha_s^2$  and  $\alpha_s^3$  given in Eq. 72 within the  $\overline{MS}$ -scheme. For this  $\overline{MS}$ -scheme expression in terms of running mass, we need the value of the RGI top mass:

$$\hat{m}_t = (254 \pm 0.4) \text{ GeV}, \quad (79)$$

deduced from Eq. 78. Adding the above expressions to the ones in the previous sections, we obtain the result given in Table 3.

<sup>6</sup>We should note that the definition of the top quark mass from different experiments is still ambiguous.

## 11. Conclusion for $a_\mu|_{l.o}^{hvp}$ and extension to $a_\tau|_{l.o}^{hvp}$

### • Results for $a_\mu|_{l.o}^{hvp}$

We have used the sum exclusive  $e^+e^- \rightarrow \text{hadrons}$  data compiled by PDG  $\oplus$  some resonances to extract the lowest order vacuum polarization contribution to the muon anomaly. We find from Table 3:

$$a_\mu|_{l.o}^{hvp} = (7036.5 \pm 38.9) \times 10^{-11}, \quad (80)$$

where the largest contribution and error come (as expected) from the  $\rho$ -meson low-energy one. It is amazing that the central value remains stable when comparing it with our old results in Refs. [17–20] though the accuracy has increased by a huge factor of about 24 (!) thanks to the experimental efforts for improving the data during about half century ! The total sum is slightly larger than the recent data based determinations in Refs. [72, 73]<sup>7</sup> but in better agreement with a recent analysis of  $\tau$ -decay data [74] and with some recent lattice results [75–77]. Using this value into Table 8 of Ref. [78] and in Table 1 of Ref. [76] where some other sources of contributions are reviewed, we deduce:

$$a_\mu^{exp} = 1165911898(42) \times 10^{-11}. \quad (81)$$

This leads to:

$$\Delta a_\mu \equiv a_\mu^{exp} - a_\mu^{th} = (142 \pm 42_{th} \pm 41_{exp}) \times 10^{-11}, \quad (82)$$

which reduces the tension between experiment and the SM prediction. We have used the experimental average from BNL [79] and FNAL [80]:

$$a_\mu^{exp} = 116592040(41) \times 10^{-11}. \quad (83)$$

### • Some comments on the determination of $a_\mu|_{l.o}^{hvp}$

◊ Instead of our simple Breit-Wigner parametrization of pion form factor done in previous sections, we have subdivided the region below 0.993 GeV to have a better fit of the data which is necessary for the extraction of the lepton anomalies. We have compared our result in this region with the ones from different experimental groups quoted in Fig 17.

◊ Our analysis differs from the most recent ones in Refs. [72, 73] as we fit the sum of exclusive modes except the  $\rho$ -meson. For the narrow resonances we use the NWA.

◊ We notice that compared to the existing analysis, we have also studied in details the contributions from the heavy quark sectors taking into account all possible resonances and, in particular, analyzed carefully the charmonium region.

◊ We have also carefully parametrized the QCD continuum contributions taking into account higher order PT quark mass corrections and the non-perturbative ones.

---

<sup>7</sup>Some earlier references are quoted in these papers and in [19].



◊ Comparing our results with the most recent ones in Refs. [72, 73], we found that in the low-energy region below 1.875 GeV, our result is higher by about  $(100 - 136) \times 10^{-11}$  than the ones in these references. This can be due to the pion form factor where we use the new data of CMD3  $\oplus$  PDG which leads to higher value of  $a_\mu$  than some other determinations as shown in Fig.17 for e.g. the region  $0.60 \leq \sqrt{t} \leq 0.88$  GeV.

◊ In the high-energy region  $\sqrt{t} \geq 1.875$  GeV, our result is  $(545.3 \pm 2.2) \times 10^{-11}$  which is about the same as the one  $(535.5 \pm 7.0) \times 10^{-11}$  of Ref. [72] but smaller by about  $38 \times 10^{-11}$  than  $(583.6 \pm 3.3) \times 10^{-11}$  in Ref. [73]. This difference is mainly due to the choice of the QCD continuum threshold  $\sqrt{t_c} = 1.8$  GeV in Ref. [73] which is lower than the one found from the asymptotic coincidence of the two sides of  $\mathcal{L}_0$  Laplace moment in Eq. 28 and requested by duality from FESR in Eq. 31.

• *Extension to the determination of  $a_\tau|_{l.o}^{hvp}$*

◊ The muon analysis has been extended to the case of the  $\tau$ -lepton by simply changing the lepton mass. The total sum is from Table 3 :

$$a_\tau|_{l.o}^{hvp} = (3494.8 \pm 24.7) \times 10^{-9}, \quad (84)$$

which we consider as an improvement of the *pioneer determination* of this quantity and of  $a_\tau$  in Ref. [20].

◊ One can notice that the relative weight of the light quarks over the heavy ones moves from 23 to 6 from  $\mu$  to  $\tau$  indicating that a measurement of the  $\tau$ -anomaly will probe higher energy region thanks to the behaviour of the QED kernel function given in Eq. 64.

◊ Our result is slightly lower than the one of Ref. [72] where the origin may come from the  $I = 0$  light mesons region.

## 12. Determination of $\Delta\alpha_{had}^{(5)}(M_Z^2)$

We conclude the paper by updating our previous determination of  $\Delta\alpha_{had}^{(5)}(M_Z^2)$  in Ref. [21]. The hadronic contribution to this quantity can be expressed as:

$$\Delta\alpha_{had}^{(5)}(M_Z^2) = - \left( \frac{\alpha}{3\pi} \right) M_Z^2 \int_{4m_\pi^2}^{\infty} \frac{R_{ee}(t)}{t(t - M_Z^2)}, \quad (85)$$

where  $R_{ee}$  is the ratio of the  $e^+e^- \rightarrow \text{Hadrons}$  over the  $e^+e^- \rightarrow \mu^+\mu^-$  total cross-sections. The results from different regions are shown in Table 3 where at the  $Z_0$  pole, we take the principal value of the integral which we take as:

$$\int_{4m_\pi^2}^{(M_Z - \Gamma_Z/2)^2} dt f(t) + \int_{(M_Z + \Gamma_Z/2)^2}^{\infty} dt f(t), \quad (86)$$

where  $\Gamma = 2.5$  GeV is the total hadronic  $Z$ -width. We add to the QCD continuum contribution the one of the  $Z$ -pole estimated to be [81]:

$$\Delta\alpha_{had}^{(5)}|_{M_Z} = 29.2 \times 10^{-5}. \quad (87)$$

Then, we obtain the total sum:

$$\Delta\alpha_{had}^{(5)}(M_Z^2) = (2766.3 \pm 4.5) \times 10^{-5}. \quad (88)$$

This value is comparable with the ones in the literature reviewed e.g. in Ref. [82]. It improves and confirms our previous determination in Ref. [21].

### 13. Summary

#### • *QCD parameters*

In the first sections, we have used the  $I = 1$  isovector component of the  $e^+e^- \rightarrow \text{Hadrons}$  data to extract, from the ratio  $\mathcal{R}_{10}$  of Laplace sum rules, the values of the four-quark and dimension  $D = 8$  condensates appearing in the OPE using as input the value of the gluon condensate  $\langle\alpha_s G^2\rangle$  (see Eq. 37).

◊ We found the value in Eq. 39 where the one of the four-quark condensate is larger by a factor about 6 than the vacuum saturation estimate. We also show that a simultaneous use of the standard SVZ value of the gluon condensate and the vacuum saturation estimate of the four-quark condensate is inconsistent.

◊ Using the value of the  $d = 6$  and  $d = 8$  condensates into the ratio  $\mathcal{R}_{10}$ , we extract the value of  $\langle\alpha_s G^2\rangle$  in Eq. 41 which is perfectly consistent with the one in Eq. 11 from heavy quarkonia.

◊ Using the previous values of the condensates, we extract  $\alpha_s$  from the lowest  $\tau$ -decay moment at different scale and found the values in Eq. 56 within FO/CI perturbation theory. This value is in good agreement with the ones from higher  $\tau$ -like decay moments within FO/CI [51].

#### • *SM-High-Precision parameters*

We complete our analysis by extracting some high-precision standard model (SM) parameters using the sum of exclusive  $e^+e^- \rightarrow \text{Hadrons}$  data.

◊ We obtain the values of the lowest order hadronic vacuum polarisation to the muon and tau anomalies  $a_\mu|_{l.o}^{hvp}$  and  $a_\tau|_{l.o}^{hvp}$  in Table 3. ◊ We determine the hadronic contribution to the running QED coupling  $\Delta\alpha_{had}^{(5)}(M_Z^2)$  in Table 3. We discuss the sources of difference of our results with the most recent determinations.

Combined with some other contributions, these results are useful for a high-precision determination of the lepton anomalies  $a_{\mu,\tau}$  and the running QED coupling  $\alpha(M_Z^2)$ . In particular, using the other sources of contributions to  $a_\mu^{th}$  from Table 8 of Ref. [78] and the updated review in Ref. [76], we obtain the result in Eq. 82 which decreases the tension between the SM prediction and experiment.

## 14. Notes added

- *Muon anomalous magnetic moment  $a_\mu$*

After the publication of this work, a new experimental measurement of the anomaly:  $a_\mu \equiv \frac{1}{2}(g-2)_\mu$  of a positive charged muon has been published [83]. This has lead to a new value of the comparison between the SM prediction and experiment [84]:

$$\Delta a_\mu \equiv a_\mu^{exp} - a_\mu^{th} = (143 \pm 42_{th} \pm 22_{exp}) \times 10^{-11}, \quad (89)$$

which indicates about  $3\sigma$  discrepancy. This number updates the one quoted in the Abstract and in Eq. 82.

- *QCD power corrections and  $\alpha_s$*

The estimate of power corrections has been recently improved by a combined use of the ratio of Laplace Sum Rule (LSR) and  $\tau$ -like decay high-moments [85]. This analysis leads to the values of the gluon  $\langle \alpha_s G^2 \rangle$ , and  $d_6$ ,  $d_8$  condensates given in Table 1 of Ref. [85]. With the new values of  $d_6$  and  $d_8$ , the ones of  $\alpha_s(M_\tau)$  to order  $\alpha_s^4$  quoted in the abstract and in Eqs. 56 to 60 becomes the one in Eqs. 30 and 31 of Ref. [85]. The increase of the value of  $d_6$  has slightly decreased the one of  $\alpha_s$ . To order  $\alpha_s^4$ , one obtains:

$$\begin{aligned} \alpha_s(M_\tau) &= 0.3081(49)_{fit}(71)_{\alpha_s^5} \implies \alpha_s(M_Z) = 0.1170(6)(3)_{evol} & \text{(FO)} \\ &= 0.3260(47)_{fit}(62)_{\alpha_s^5} \implies \alpha_s(M_Z) = 0.1192(6)(3)_{evol} & \text{(CI),} \end{aligned} \quad (90)$$

where the sum of non-perturbative corrections at the  $\tau$ -mass is:  $\delta^{(NP)} = (3.8 \pm 0.8) \times 10^{-2}$  (Table 3 of Ref. [85]). The previous values lead to the mean:

$$\alpha_s(M_\tau)|_{SVZ} = 0.3194(52)(113)_{syst} \implies \alpha_s(M_Z)|_{SVZ} = 0.1184(15)(3)_{evol}, \quad (91)$$

where the systematics is the distance between the mean central value to the FO/CI ones.

## Acknowledgement

We thank Antonio Pich and Eduardo de Rafael for some correspondences.

## References

- [1] M.A. Shifman, A.I. Vainshtein, V.I. Zakharov, *Nucl. Phys.* **B147** (1979) 385; *ibid*, *Nucl. Phys.* **B147** (1979) 448.
- [2] S. Narison and E. de Rafael, *Phys. Lett.* **B 103**, (1981) 57.
- [3] J.S. Bell and R.A. Bertlmann, *Nucl. Phys.* **B177**, (1981) 218; *Nucl. Phys.* **B187**, (1981) 285.
- [4] V.I. Zakharov, *Int. J. Mod .Phys.* **A14**, (1999) 4865.
- [5] S. Narison, *QCD spectral sum rules*, *World Sci. Lect. Notes Phys.* **26** (1989) 1.
- [6] S. Narison, *QCD as a theory of hadrons*, *Cambridge Monogr. Part. Phys. Nucl. Phys. Cosmol.* **17**. (2004) 1-778 [hep-ph/0205006].
- [7] S. Narison, *Nucl. Part. Phys. Proc.* **312-317** (2021) 87;
- [8] S. Narison, *Nucl. Part. Phys. Proc.* **258-259** (2015) 189.
- [9] S. Narison, *Phys. Rept.* **84** (1982) 263; S. Narison, *Acta Phys. Pol.* **B 26**(1995) 687; S. Narison, *Riv. Nuovo Cim.* **10N2** (1987) 1; S. Narison, *Nucl. Part. Phys. Proc.* **207-208**(2010) 315.
- [10] L.J. Reinders, H.R. Rubinstein, S. Yazaki, *Phys. Reports* **127** (1985) 1.
- [11] E. de Rafael, les Houches summer school, hep-ph/9802448 (1998).
- [12] R.A. Bertlmann, *Acta Phys. Austriaca* **53**, (1981) 305.
- [13] F.J Yndurain, *The Theory of Quark and Gluon Interactions*, 3rd edition, Springer, New York (1999).
- [14] P. Pascual and R. Tarrach, *QCD: renormalization for practitioner*, Springer, New York (1984).
- [15] H.G. Dosch, *Non-pertubative Methods*, ed. Narison, World Scientific, Singapore (1985).
- [16] P. Colangelo, A. Khodjamirian, *At the Frontier of Particle Physics: Handbook of QCD*, **1495**, edited by M. Shifman (World Scientific, Singapore, 2001).
- [17] J. Calmet, S. Narison, M. Perrottet and E. de Rafael, *Phys. Lett.* **B161** (1976) 283; *Rev. Mod. Phys.* **49** (1977)21.
- [18] S. Narison, *Thèse de 3 ème cycle*, Univ. Marseille Luminy (1976) unpublished.
- [19] S. Narison, *Phys. Lett.* **B513** (2001) 53; *Phys. Lett.* **B526** (2002) 414 (erratum).
- [20] S. Narison, *J. Phys.: Nucl. Phys.* **G4** (1978) 1849.
- [21] S. Narison, arXiv: 0108065[hep-ph] (2001).

- [22] R. Tarrach, *Nucl.Phys.* **B 196** (1982) 45.
- [23] D. Espriu and R. Tarrach, *Z. Phys.* **C 16**, (1982) 77.
- [24] S. Narison, R. Tarrach, *Phys. Lett.* **B125** (1983) 217; M. Jamin, M. Kremmer, *Nucl. Phys.* **B277** (1986) 349.
- [25] E. Bagan, J.I. Latorre, P. Pascual, R. Tarrach, *Nucl. Phys.* **B254** (1985) 555.
- [26] S.G. Gorishny, A.L. Kataev, S.A. Larin, *Phys. Lett.* **B259** (1991) 144; L.R. Surguladze, M.A. Samuel, *Phys. Rev. Lett.* **66** (1991) 560.
- [27] P. A. Baikov, K.G. Chetyrkin, J.H. Kühn, *Phys.Rev.Lett.* **101**(2008) 012002.
- [28] K.G. Chetyrkin, S. Narison and V.I. Zakharov, *Nucl. Phys.* **B550** (1999) 353.
- [29] S. Narison and V.I. Zakharov, *Phys. Lett.* **B679** (2009) 355.
- [30] S. Narison and V.I. Zakharov, *Phys. Lett.* **B522** (2001) 266.
- [31] For reviews, see e.g.: V.I. Zakharov, *Nucl. Phys. Proc. Suppl.* **164** (2007) 240; S. Narison, *Nucl. Phys. Proc. Suppl.* **164** (2007) 225.
- [32] O. Andreev, *Phys. Rev.* **D73** (2006) 107901; O. Andreev, V.I. Zakharov, *Phys. Rev.* **D74** (2006) 025023; *ibid*, **D76** (2007)047705.
- [33] F. Jugeau, S. Narison, H. Ratsimbarison, *Phys. Lett.* **B722** (2013) 111.
- [34] S. Narison, *Phys. Lett.* **B300** (1993) 293
- [35] S. Narison, *Phys. Lett.* **B361** (1995) 121;
- [36] S. Narison, *Phys. Lett.* **B673** (2009) 30.
- [37] M. Kozhevnikova, A. Oganesian and O. Terayev, EPJ Web of Conferences 204 (2019) 02005.
- [38] S. Narison, *Int. J. Mod. Phys.* **A33** (2018) no. 10, 185004; Addendum: *Int. J. Mod. Phys.* **A33** (2018) no.10, 1850045.
- [39] W. Hubschmid, S. Mallik, *Nucl. Phys.* **B207**, (1982) 29; M.S. Dubovikov, A.V. Smilga, *Nucl. Phys.* **B185**, (1981) 109.
- [40] D. Broadhurst, S. Generalis, *Phys. Lett.* **B165** (1985) 175.
- [41] R.A. Bertlmann, G. Launer and E. de Rafael, *Nucl. Phys.* **B250**, (1985) 61; R.A. Bertlmann, C.A. Dominguez, M. Loewe, M. Perrottet and E. de Rafael, *Z. Phys.* **C39** (1988) 231.
- [42] G. Launer, S. Narison, R. Tarrach, *Z. Phys.* **C26** (1984) 433.

- [43] R.L. Workman et al. (Particle Data Group), *Prog. Theor. Exp. Phys.* **2022** (2022) 083C01.
- [44] CMD-3 Collaboration - F.V. Ignatov et al., 2302.08834 [hep-ex] (2023).
- [45] M.S.A Alam Kahn (private communication).
- [46] D. Boito, S. Carlos. M. Golterman, K. Maltman, S. Peris, M.V. Rodrigues, arXiv: 2112.05413 [hep-ph] (2021) and references quoted therein.
- [47] The ALEPH Collaboration-R. Barate et al., *Eur. Phys. J.* **C4** (1998) 409.
- [48] The OPAL Collaboration-K. Ackerstaff et al., *Eur. Phys. J.* **C7** (1999) 571.
- [49] A. Pich, A. Rodriguez-Sanchez, *Phys.Rev.* **D94** (2016) 3, 034027.
- [50] M. Davier, A. Höcker, B. Malaescu, C. Z. Yuan, Z. Zhang, *Eur. Phys. J.* **C74** (2014) 2803.
- [51] A. Pich, A. Rodriguez-Sanchez, *Mod.Phys.Lett.* **A31** (2016) 30, 1630032; *Journal of High Energy Physics* **145** (2022).
- [52] F. Le Diberder, A. Pich, *Phys. Lett.* **B286** (1992) 147; **B289** (1992) 165.
- [53] E. Braaten, *Phys. Rev. Lett.* **60** (1988) 606; E. Braaten, *Phys. Rev.* **D39** (1989) 1458; S. Narison, A. Pich, *Phys. Lett.* **B211** (1988) 183.
- [54] E. Braaten, S. Narison, A. Pich, *Nucl. Phys.* **B373** (1992) 581.
- [55] C.A. Dominguez, J. Sola, *Z. Phys.* **C40** (1988) 63.
- [56] J. Bordes, V. Gimenez, J.A. Penarrocha, *Phys. Lett.* **B201** (1988) 365.
- [57] M.B. Causse, G. Mennessier, *Z. Phys.* **C47** (1990) 611.
- [58] S.I. Eidelman, L.M. Kurdadze, A.I. Vainshtein, *Phys. Lett.* **B82** (1979) 278.
- [59] M.S.A. Alam Khan, arXiv: 2306.10262 (2023).
- [60] S. Narison, A. Pich, *Phys. Lett.* **B304** (1993) 359.
- [61] M. A. Benitez-Rathgeb, D. Boito, A.H. Hoang, M. Jamin, *JHEP* **09** (2022) 223; *ibid* **07** (2022) 016.
- [62] M. Beneke, M. Jamin, *JHEP* **044** (2008) 0809.
- [63] C. Ayala, G. Cvetič, D. Teca, *Eur. Phys. J.* **C81** (2021) 930.
- [64] C. Bouchiat and L. Michel, *J. Phys. Radium* **22** (1961) 121.
- [65] L. Durand III, *Phys. Rev.* **128** (1962) 441; erratum **129** (1963) 2835.

- [66] T. Kinoshita and R. Oakes, *Phys. Lett.* **B25**(1967) 143.
- [67] J.E. Bowcock, *Z. Phys.* **211** (1968) 400.
- [68] M. Gourdin and E. de Rafael, *Nucl. Phys.* **B10** (1969) 667.
- [69] B. Lautrup and E. de Rafael, *Phys. Rev.* **174** (1968) 1835.
- [70] K.G. Chetyrkin, J.H. Kühn, A. Kwiatkowski, *Phys. Lett.* **B282** (1992) 221; K.G. Chetyrkin, J.H. Kühn, *Nucl. Phys.* **B432** (1994) 337.
- [71] E.G. Floratos, S. Narison, E. de Rafael, *Nucl. Phys.* **B155** (1979) 115.
- [72] A. Keshavarzi, D. Nomura, T. Teubner, *Phys. Rev.* **D101** (2020) 014029.
- [73] M. Davier, A. Höcker, B. Malaescu, Z. Zhang, *Eur. Phys. J.* **C80** (2020) 241.
- [74] P. Masjuan, A. Miranda, P. Roig, arXiv:2305.20005 (2023) and private communication from A. Miranda.
- [75] E. de Rafael, *Phys. Lett.* **B736** (2014) 522.
- [76] T. Aoyama et al., *Phys. Rept.* **887** (2020)1 and references therein.
- [77] Sz. Borsanyi et al. *Nature* **593(7857)** (2021)51; Marco C'è et al., *Phys. Rev.* **D106(11)** (2022)114502; C. Alexandrou et al., *PoS ICHEP 2022* (2022) 794; T. Blum et al., arXiv: 2301.08696 [hep-lat] (2023).
- [78] M. Knecht, S. Narison, A. Rabemananjara, D. Rabetiarivony *Phys. Lett.* **B787** (2018) 111.
- [79] G. Bennett et al., *Phys. Rev.* **D73** (2006) 072003.
- [80] B. Abi et al., *Phys. Rev. Lett.* **126** (2021) 141801; T. Albahri et al., *Phys. Rev.* **D103** (2021) 072002.
- [81] J. F. de Troconiz, F. J. Yndurain, *Phys. Rev.* **D65** (2002) 093002.
- [82] F. Jegerlehner, *CERN Yellow Reports: Monographs* **3** (2020) 9.
- [83] D.P. Aguillard et al., *Phys. Rev. Lett.* **131** (2023) 16, 161802.
- [84] S. Narison, talk given at QCD2023 (10-14 july 2023, Montpellier-FR), arXiv: 2309.05342 [hep-ph], *Nucl. Part. Phys. Proceedings* (in press).
- [85] S. Narison, arXiv: 2402.13983 [hep-ph] (2024).